

Review

Engineering Rational SERS Nanotags for Parallel Detection of Multiple Cancer Circulating Biomarkers

Zhipeng Zhang ^{1,†}, Rui Guan ^{2,3,†}, Junrong Li ^{2,4}  and Yao Sun ^{2,*}

¹ Xianning Medical College, College of Pharmacy, Hubei University of Science & Technology, Xianning 437100, China

² Key Laboratory of Pesticide and Chemical Biology, Ministry of Education, College of Chemistry, Central China Normal University, Wuhan 430072, China

³ Key Laboratory for Analytical Science of Food Safety and Biology, Ministry of Education, Fuzhou University, Fuzhou 350108, China

⁴ Key Laboratory of Optic-Electric Sensing and Analytical Chemistry of Life Science, Ministry of Education, Qingdao University of Science and Technology, Qingdao 266061, China

* Correspondence: sunyaogbasp@ccnu.edu.cn

† These authors contributed equally to this work.

Abstract: Precision cancer medicine necessitates a personalized treatment plan for each individual patient. Given cancer's heterogeneity and dynamic nature, the plot of patient-specific signatures composed of multiple cancer circulating biomarkers is useful to reveal the complete tumor landscape for guiding precision medicine. As an emerging new technology, surface-enhanced Raman scattering (SERS) shows the intrinsic advantage of performing multiplexed detection with the extremely narrow Raman spectral line widths. In this review, we first discuss the design principle of SERS nanotags to enable the detection of multiple circulating biomarkers, highlighting the important roles of plasmonic nanostructures and triple bond-modulated Raman reporters. Following this, we detail the use of isotropic and anisotropic nanostructures as SERS enhancement substrates for amplifying Raman signals in multi-biomarker detection. Furthermore, we present the triple bond-modulated molecules as Raman reporters in SERS nanotags to expand the multiplexing capability for biomarker measurements. Finally, we offer critical insights into the challenges and perspectives of SERS nanotags for cancer diagnosis, particularly from the aspect of future clinical transition. It is expected that this review can facilitate the design of more functional SERS nanotags with high sensitivity and multiplexing capability to assist early and accurate cancer screening. We also believe our review will be of interest in the fields of molecular imaging, biomedicine, and analytical chemistry.

Keywords: SERS; Raman; nanotages; cancer diagnosis



Citation: Zhang, Z.; Guan, R.; Li, J.; Sun, Y. Engineering Rational SERS Nanotags for Parallel Detection of Multiple Cancer Circulating Biomarkers. *Chemosensors* **2023**, *11*, 110. <https://doi.org/10.3390/chemosensors11020110>

Academic Editors: Xiaobing Zhang, Lin Yuan and Guoliang Ke

Received: 29 December 2022

Revised: 1 February 2023

Accepted: 1 February 2023

Published: 3 February 2023



Copyright: © 2023 by the authors. Licensee MDPI, Basel, Switzerland. This article is an open access article distributed under the terms and conditions of the Creative Commons Attribution (CC BY) license (<https://creativecommons.org/licenses/by/4.0/>).

1. Introduction

As the leading cause of death worldwide, cancer is responsible for nearly 10 million deaths in 2020 [1]. Fortunately, emerging findings suggested that precision medicine can significantly reduce cancer mortality through introducing timely and effective medical interference [2–5]. To assist precision medicine, biomarkers circulating in body fluids (e.g., blood or urine) are able to noninvasively provide a complete cancer profile to enable early detection and guide personalized treatment management [6–8]. Currently, a variety of cancer circulating biomarkers has been investigated as surrogates to indicate cancer occurrence, progression, and treatment response, including proteins, circulating tumor cells (CTCs), nucleic acids (NAs), and extracellular vesicles (EVs) [9–12].

Despite the significant role of circulating biomarkers in cancer detection, their practical use for precision medicine is largely challenged by two issues: (1) the extremely low abundance of cancer-associated circulating biomarkers in the presence of large amounts of interference molecules. For instance, only 1–100 CTCs are found in one milliliter of

blood with 1–2 million peripheral blood mononuclear cells, in which CTCs may experience further loss during the isolation and purification procedures [13,14], and (2) the inaccurate reflection of cancer status by considering only one relevant biomarker. Accumulating evidence shows that the mere use of prostate-specific antigen (PSA) for prostate cancer screening may not produce an improved survival benefit but comes with overtreatments and life-altering side effects [15,16]. As such, new technologies that enable highly sensitive, specific, and parallel analysis of multiple circulating biomarkers are expected to assist accurate decision-making [2,17].

Surface-enhanced Raman scattering (SERS) is an emerging spectroscopic technology that has witnessed rapid developments in the past decade [18]. By integrating with nanotechnology (e.g., noble metal nanoparticles), SERS allows 10^6 – 10^{15} Raman signal amplification and thus sensitive sensing down to single molecules [19]. In addition, SERS possesses extremely narrow Raman spectral line widths (i.e., ~ 1 nm), which are about 50 times narrower than the commonly used fluorescence bands [19]. The intrinsic narrow Raman peaks particularly benefit multiplexed labeling with the potential to analyze 31 targets in parallel [20]. Taken together, with the advantages of high sensitivity and multiplexing capability, SERS is a good candidate to implement circulating biomarker detection for early and accurate cancer detection.

In this review, we feature the use of the SERS technique, particularly SERS nanotags, to detect cancer circulating biomarkers in a highly sensitive and multiplexed way (Figure 1). We first deliberate on the SERS nanotag design principle. Following that, we focus on the SERS nanotags using isotropic or anisotropic nanostructures as plasmonic nanostructures to enhance Raman signals for highly sensitive biomarker detection. Furthermore, we discuss the SERS nanotags with the use of triple bond-modulated Raman reporters to expand the multiplexing detection. Finally, we provide our insights on the current challenges and outlooks of SERS technique in cancer detection. This review will help researchers in the fields of Raman imaging, nanomedicine, and biomedicine to develop promising Raman agents for cancer early diagnosis and therapy.

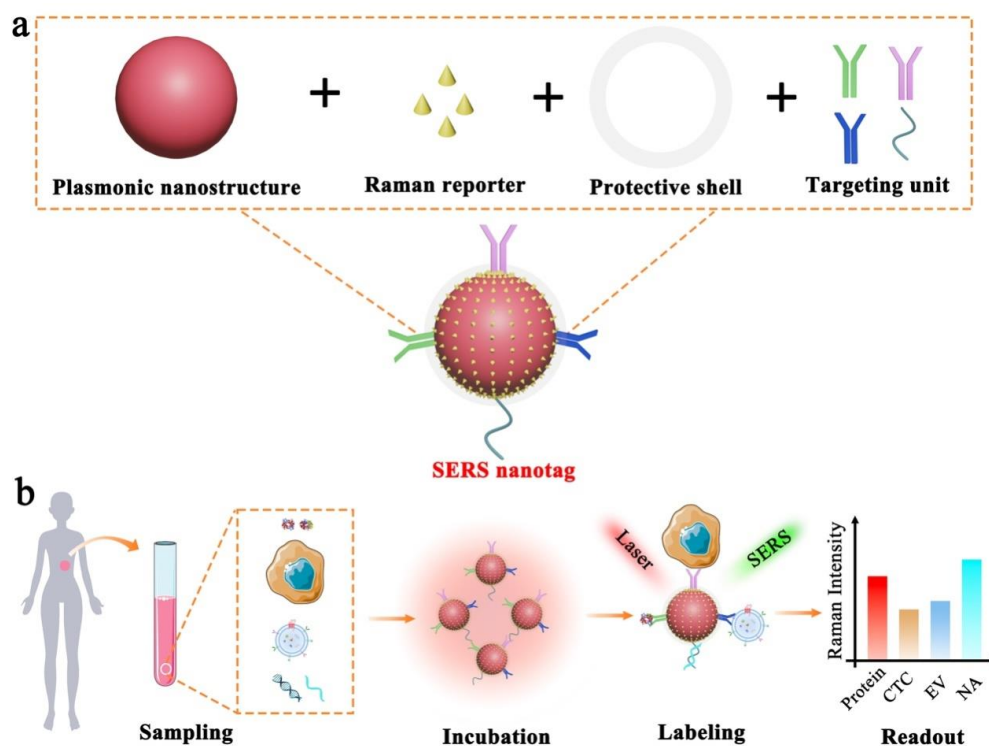


Figure 1. Schematic illustration of SERS nanotag enabled highly sensitive and multiplexed detection of cancer circulating biomarkers. (a) The design of a typical SERS nanotag with the use of four key components. (b) The application of SERS nanotags in the detection of protein, CTC, EV, and NA.

2. The Design Principle of SERS Nanotags

Figure 2 depicts the electromagnetic field-related SERS principle, which involves the use of surface plasmonic resonance (SPR) surrounding nanostructure surfaces to enhance the Raman signals of Raman reporters. To allow effective biomarker detection, SERS nanotags are expected to identify the targets as well as readout specific signals. Typically, the design of SERS nanotags should consider four key components, as illustrated in Figure 1a: (1) plasmonic nanostructure, (2) Raman reporter, (3) protective shell, and (4) targeting unit. The integration of these four parts together constitutes the functional SERS nanotags. Table 1 summarizes the roles of each component, typical examples, and working principles.

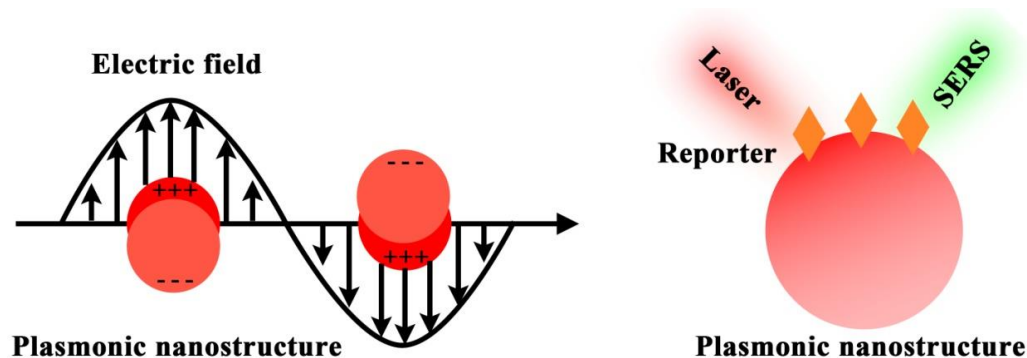


Figure 2. SERS principle of using plasmonic nanostructure to enhance the Raman reporter signals.

Table 1. Typical components of functional SERS nanotags.

Component	Role	Example	Working Principle
Plasmonic nanostructure	Enhancing Raman signals	<ul style="list-style-type: none"> • Gold/silver nanospheres • Gold/silver nanostars/nanoboxes 	Localized surface plasmon resonance (LSPR)
Raman reporter	Generating Raman signals	<ul style="list-style-type: none"> • 4-Mercaptobenzoic acid • 2,3,5,6-tetrafluoro-4-mercaptobenzoic acid • 5,5-dithio-bis-(2-nitrobenzoic acid) • Crystal violet • 4-Cyanobenzenethiol • 4-mercaptopyridine • 2-mercapto-4-methyl-5-thiazoleacetic acid • Rhodamine 6G 	Intrinsic molecular vibration and rotation
Protective shell	<ul style="list-style-type: none"> • Preventing Raman reporter from detaching • Maintaining nanostructure stability • Reducing non-specific binding 	<ul style="list-style-type: none"> • Bovine serum albumin (BSA) • SH-PEG • SiO₂ • Liposome 	<ul style="list-style-type: none"> • Physical isolation • Steric hindrance/repulsive force • Block free and high-energy nanostructure surface
Targeting unit	Providing required specificity	<ul style="list-style-type: none"> • Antibody • Aptamer • Nucleic acid • Peptides • Small ligands 	Specific molecular interactions

As the foundation of SERS nanotags, the plasmonic nanostructure plays a paramount role in amplifying the weak Raman signals, which underpins the feasibility of single-molecule detection. Briefly, the plasmonic nanostructure utilizes the localized surface plasma resonance (LSPR) to enhance the surrounding electromagnetic field and thus enlarge the molecular vibrational and rotational information [21,22]. Due to the electromagnetic field damping with the distance away from the nanostructures, this LSPR-based Raman enhancement shows the distance-dependent feature with effective signal enhancement limited to around 10 nm near the nanostructure surfaces [23]. Typically, plasmonic nanostructure consists of noble metals (e.g., gold, silver, and copper) that show strong LSPR properties. Importantly, plasmonic nanostructure with different morphology shows variable electromagnetic field distributions and thus quite diverse LSPR-related Raman signal enhancement [24–26]. For instance, plasmonic nanostructure that is isotropic (e.g., nanospheres) or anisotropic (e.g., nanostars and nanoflowers) performs differently in enhancing Raman signals. Based on these different morphology, scientists could design promising Raman probes for *in vitro* and *in vivo* imaging.

Raman reporter provides the intrinsic fingerprint molecular information, which can be used as characteristic signals to indicate targets. As Raman peaks are extremely narrow, the use of different Raman reporters with non-overlapping characteristic bands is capable of labeling multiple targets in parallel. Typically, the thiolated small molecules (e.g., 4-mercaptobenzoic acid, 2,7-mercapto-4-methylcoumarin, 4-mercaptopyridine, and 2-mercapto-4-methyl-5-thiazoleacetic acid) are preferred Raman reporters in multi-biomarker analysis due to their easy functionalization on nanostructures through sulfur and gold/silver interaction and few characteristic peaks to minimize Raman peak overlaps [19]. However, this type of molecules suffers from a relatively low Raman signal enhancement, which is largely related to their small Raman-scattering cross-section. By contrast, the dye-based Raman reporters (e.g., crystal violet and rhodamine B) feature high Raman enhancement but have the limitation of serious Raman peak overlap due to the complex molecular structures with rich vibration and rotation [19]. Thus, these dyes as Raman reporters are recommended to conduct the highly sensitive detection of an individual biomarker instead of the simultaneous analysis of multi-biomarkers. In addition, the emerging triple bond-modulated molecules are attracting an increasing attention as the next generation of Raman reporters for multiplexed biomarker detection. These triple bond-based molecules show unique and simple Raman signals beyond 1800 cm^{-1} , which locate in the Raman silent region without potential interferences from biological samples [27].

A protective shell is used to prevent the dissociation of Raman reporters on nanostructure surfaces, provide sufficient colloidal stability to the nanostructures, and block the exposed free nanostructure surfaces to avoid nonspecific binding events. The representative protective materials include bovine serum albumin (BSA), SH-PEG, SiO_2 , and liposomes [28–31].

The targeting unit (e.g., antibodies, aptamers, peptides, small ligands, and nucleic acids) imparts the specificity to SERS nanotags for recognizing desired targets. The incorporation of targeting units on SERS nanotags can be performed through a simple physical adsorption using electrostatic interactions or covalent binding with the assistance of bifunctional linker molecules (e.g., ortho-pyridyldisulfide-polyethylene glycol-N-succinimidyl propionate, dithiobis(succinimidyl propionate) and succinimidyl-4-(N-maleimidomethyl)cyclohexane-1-carboxylate) [19].

To perform SERS measurements, the targets are typically isolated/purified from the samples first and identified through SERS nanotags for signal readout. Experimentally, under the laser illumination with specific wavelength (e.g., 632.8 nm and 785 nm), the generated Raman spectra are recorded with either a portable Raman instrument in a cuvette or confocal Raman microscope using user-defined integration time [32,33].

In this review, we focus on discussing the SERS nanotags that use isotropic and anisotropic nanostructures as well as triple bond-modulated Raman reporters, aiming to

achieve the goal of highly sensitive and multiplexed circulating biomarker detection for the early diagnosis of diseases.

3. Morphology-Tuned Plasmonic Nanostructures in SERS Nanotags for Multi-Biomarker Detection

As mentioned in the previous section, plasmonic nanostructure is the key component to amplify Raman signals in SERS nanotags. Particularly, the morphology of plasmonic nanostructures influences the electromagnetic field distribution and thus the Raman signal enhancement performance. Thus, in this section, we discuss two classes of nanostructures with isotropic and anisotropic shapes as Raman signal amplifiers in SERS nanotags. Isotropic nanostructures allow the change in plasmonic resonance by varying the nanoparticle sizes but typically show a relatively narrow plasmon resonance within a small wavelength range (i.e., a few tens of nanometers) [34]. Furthermore, isotropic nanostructures show a low SERS enhancement capability and thus require the nanostructure aggregation to produce “hot spots” for sufficient signal amplification [35]. This, however, will lead to the SERS signal variation as the generated “hot spots” are randomly distributed on the nanostructure surfaces [36,37], which may result in poor reproducibility in biomarker detection. In contrast, anisotropic nanostructures enable a better control of plasmon resonance wavelength due to the introduction of another degree of freedom by shape anisotropy [38,39]. With the advantage of extremely strong electromagnetic field on specific sites, anisotropic nanostructures demonstrate single-particle SERS activity without relying on aggregation [40–42]. Thus, anisotropic nanostructures are believed to provide robust and reproducible strategies for biomarker detection with high specificity and sensitivity [43].

3.1. Isotropic Nanostructures

Gold/silver nanospheres are the representative isotropic nanostructures that are most commonly used as plasmonic nanomaterials in SERS nanotags. Thus far, gold/silver nanospheres’ syntheses are well-established and their properties (e.g., size) are fully investigated to maximize the Raman signal enhancement. Here, we focus on the use of gold/silver nanosphere-based plasmonic nanostructures in SERS nanotags to detect multiple cancer circulating biomarkers.

To allow the sensitive detection and phenotypic profiling of melanoma CTCs, Tsao et al. used gold nanospheres to prepare four SERS nanotags that identified four protein biomarkers on CTCs (Figure 3a) [44]. After the blood samples were purified to remove irrelevant cells, the remaining CTCs were labeled by the four SERS nanotags and detected by Raman spectroscopy. Specifically, the four SERS nanotags targeted four corresponding biomarkers on melanoma cells, namely melanoma–chondroitin sulfate proteoglycan (MCSP), melanoma cell adhesion molecule (MCAM), erythroblastic leukemia viral oncogene homologue 3 (ErbB3), and low-affinity nerve growth factor receptor (LNGFR). These four SERS nanotags labeled melanoma CTCs and created a molecular signature of each melanoma patient, which allowed the monitoring of patient phenotypic changes during cancer treatments. Furthermore, based on either one SERS nanotag alone or four SERS nanotags together, the assay can sensitively detect melanoma CTCs down to 10 cells/mL. As a comparison, the use of a single surface biomarker for CTC isolation and detection (e.g., epithelial cell adhesion molecule (EpCAM)) was deemed to introduce bias due to the dynamic nature of CTCs that may have no expression or downregulate the expression of the specific biomarker. Thus, this work highlighted the importance of SERS nanotag enabled multi-biomarker analysis for accurate cancer diagnosis.

In a follow-up study, by changing the targeting units, Zhang and colleagues used a similar strategy to prepare four SERS nanotags based on gold nanospheres as plasmonic nanostructures (Figure 2b) [45]. Different from the above work, this research was focusing on monitoring the epithelial to mesenchymal transition (EMT) to indicate cancer metastasis by measuring the CTC surface biomarker level changes. In the breast cancer cell line

models with induced EMT process, their finding suggested the downregulation of the CTC biomarker and a mesenchymal biomarker but the upregulation of a mesenchymal biomarker and a stem cell biomarker. Importantly, the gold nanosphere-based SERS nanotags were able to detect breast cancer patients and phenotype their EMT-associated characteristics. This approach offered a new strategy to monitor EMT development in different cancer types and thus may be a useful tool to allow an early identification of cancer metastasis.

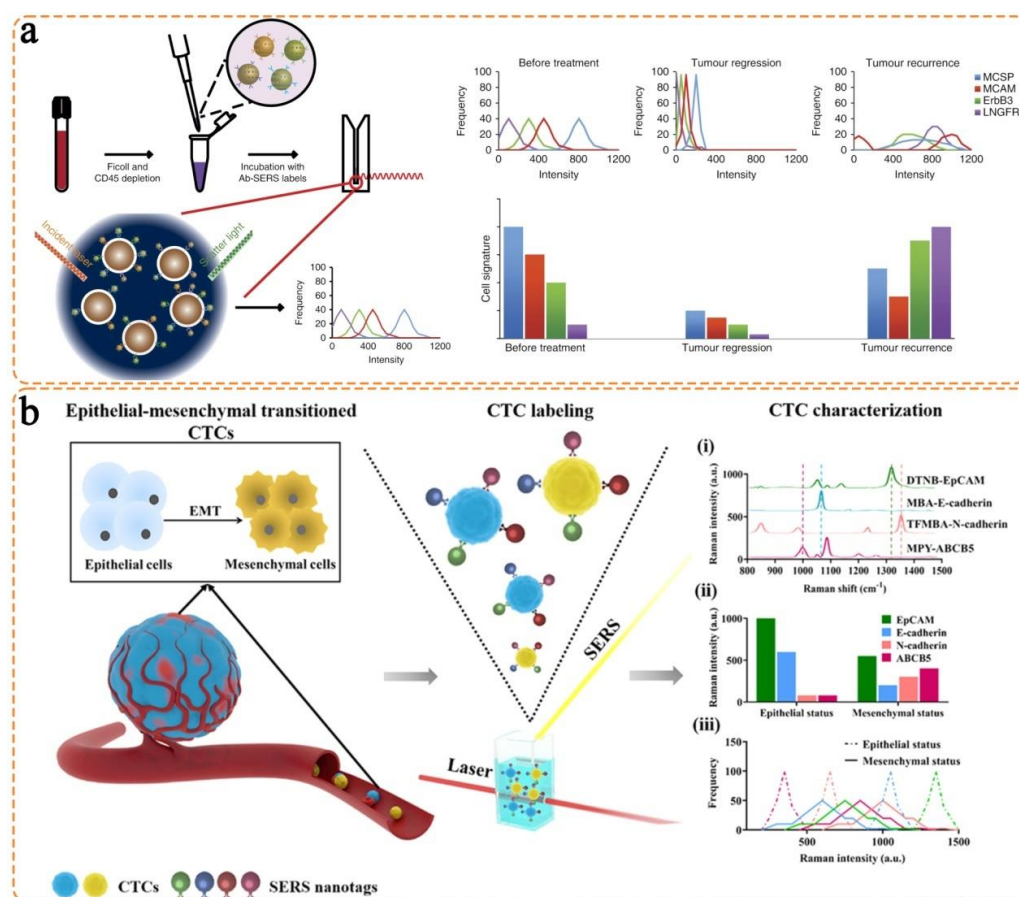


Figure 3. Gold nanosphere-based SERS nanotags for multi-biomarker detection. (a) Profiling of four biomarkers on melanoma CTC surface to monitor patients' response to drug treatments, which involved Ficoll and CD45 depletion and incubation with Ab-SERS labels for Raman detection. Reproduced with permission [44]. Copyright 2018, Nature Publishing Group. (b) Detection of four biomarkers (i.e., EpCAM, E-cadherin, N-cadherin, and ABCB5) on melanoma CTC surfaces to monitor epithelial to mesenchymal transition. Reproduced with permission [45]. Copyright 2021, American Chemical Society.

Gold nanosphere-based SERS nanotags can further integrate with microfluidic systems to improve the analytical performance in biomarker detection. For instance, Reza and coworkers first utilized gold nanospheres to prepare four SERS nanotags, which were able to detect the cancer-specific protein biomarkers circulating in blood (Figure 4a) [46]. Furthermore, a microfluidic chip was fabricated and functionalized with different capture antibodies in separate channels. The presence of the targets was able to bridge the SERS nanotags and the microfluidic surface in a sandwich structure. Importantly, this work introduced electrohydrodynamic (EHD)-induced surface shearing forces on the microfluidic system to control the fluidic flow. As a result, the interaction between the targets/SERS nanotags and the microfluidic chip was enhanced along with the significantly reduced

non-specific binding events. This work demonstrated the applications of SERS nanotags for clinical potential by testing the protein biomarkers in breast and ovarian cancer patients.

The integration of gold nanosphere-based SERS nanotags and a multi-channel microfluidic system was also used to profile protein biomarkers on EV surfaces (Figure 4b) [47]. Specifically, Wang and colleagues first prepared four SERS nanotags based on gold nanospheres, followed by applying them on the fabricated microfluidic channels to form the conventional sandwich structure and identify the target EVs. Due to the highly sensitive readout of the prepared SERS nanotags and the incorporation of the EHD for EV enrichment, this work demonstrated the direct EV profiling from plasma samples without the need for EV purification. The test in melanoma patient samples revealed that specific EV profiles can indicate drug resistance development, which can be employed to investigate cancer treatment outcomes.

Apart from the above multi-channel microfluidic devices, gold nanosphere-based SERS nanotags were used together with the ring microfluidic system for biomarker detection. For instance, Zhang et al. prepared two gold nanosphere-based SERS nanotags coupled with the ring microfluidic chip to detect two soluble EMT biomarkers (Figure 4c) [48]. The SERS nanotag preparation was conducted in a traditional approach, which was similar to the above works. However, the design of the microelectrode chip with ring shapes further improved the mixing effect (i.e., nanomixing) on the chip that accelerated the collision of gold nanosphere-based SERS nanotags and chip surfaces. As a result of this, the sensitive detection of soluble epithelial cadherin (E-cadherin) and neural-cadherin (N-cadherin) can be performed from as low as 10 cells/mL. To demonstrate the clinical usage, this work showed the successful detection of both E-cadherin and N-cadherin in the plasma samples from breast cancer patients who were diagnosed in metastatic stage IV.

In addition to integrate with microfluidic systems, gold nanosphere-based SERS nanotags can also be flexibly used with magnetic nanobeads for cancer biomarker detection. Wang and colleagues designed a SERS assay for simultaneously detecting three cancer EV biomarkers (Figure 5a) [49]. Instead of using antibodies as the targeting units, the gold nanospheres were functionalized with aptamers to recognize the protein biomarkers on EV surfaces and prepare SERS nanotags. Following the EV capture through the generic surface protein CD63 by magnetic nanobeads, the SERS nanotags were applied to identify specific biomarkers on EVs (i.e., human epidermal growth factor receptor 2 (HER2), prostate-specific membrane antigen (PSMA), and carcinoembryonic antigen (CEA)) with the formation of the apta-immunocomplexes. After isolating the apta-immunocomplexes from the solution with a magnet, the EV existence was indicated by the reduced SERS signals. Based on the obtained EV-associated SERS signals, this work achieved the screening of breast, colorectal, and prostate cancers.

Furthermore, gold nanosphere-based SERS nanotags can enhance the signal readout by coupling with silver nanospheres. Gu et al. designed a SERS biosensor to simultaneously detect alpha-fetoprotein (AFP) and CEA (Figure 5b) [50]. In this assay, through electrodeposition of gold on silica cavities, a gold microelectrode array (GMA) was fabricated and functionalized with antibodies to capture the targets. SERS nanotags were prepared by co-conjugating gold nanospheres with antibodies and capture DNA, in which the captured DNA can initiate a hybridization chain reaction (HCR) to load Raman reporters. In the presence of the desired biomarker, a conventional sandwich structure was formed between GMA and SERS nanotags. A subsequent silver staining was performed that deposited silver nanospheres on gold nanosphere-based SERS nanotags. The electromagnetic coupling between gold and silver nanospheres enabled ultrasensitive detection of AFP and CEA down to 0.6 and 0.3 pg/mL, respectively. Apart from SERS readout, this design also allowed the quantification of biomarkers with electrochemical signals.

As discussed above, the majority of studies preferred to use gold instead of silver as the basic material in nanostructures to enhance Raman signals. As a popular noble metal, gold has the advantages of high stability and it is easy to tune the morphology in a controlled manner, but pure gold has the slightly lower Raman enhancement capability. In contrast, though silver is reported to produce a much higher Raman enhancement than

gold, the poor stability and the difficulty to control the nanostructure uniformity limit their practical use as SERS plasmonic nanostructures in nanotag design, particularly for the application in biomarker detection. To integrate the advantages of gold and silver together, the design of gold–silver alloys or core–shell nanostructures is a promising direction. Such novel nanostructures are expected to possess the required physical stability and generate significantly enhanced Raman signals due to the electromagnetic coupling effect between gold and silver components, which will greatly benefit the robust and sensitive detection of rare circulating biomarkers.

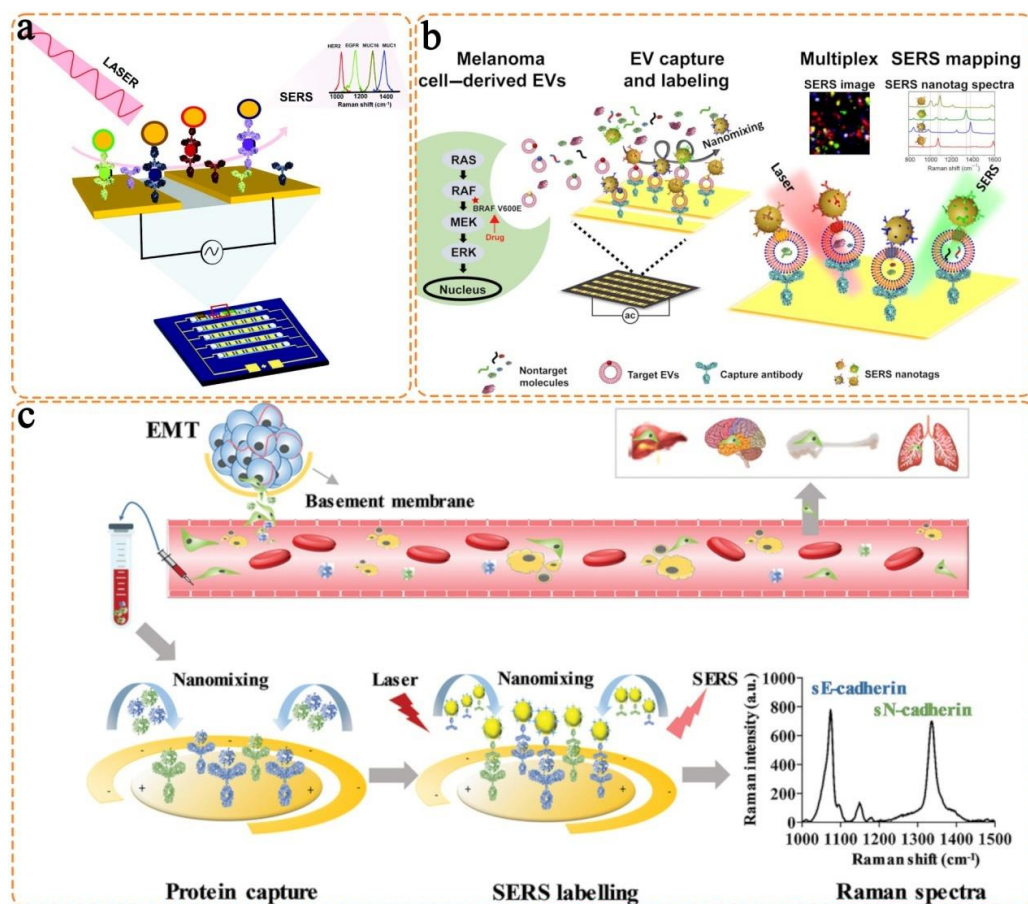


Figure 4. Integration of gold nanosphere-based SERS nanotags with microfluidic systems for multi-biomarker detection. (a) Detection of four circulating protein biomarkers (i.e., HER2, EGFR, MUC16, and MUC1). Reproduced with permission [46]. Copyright 2017, Wiley-VCH. (b) Profiling of four EV biomarkers from melanoma cell derived EVs. Reproduced with permission [47]. Copyright 2020, American Association for Advancement Science. (c) Measurement of two circulating protein biomarkers (i.e., sE-cadherin and sN-cadherin). Reproduced with permission [48]. Copyright 2020, Wiley-VCH.

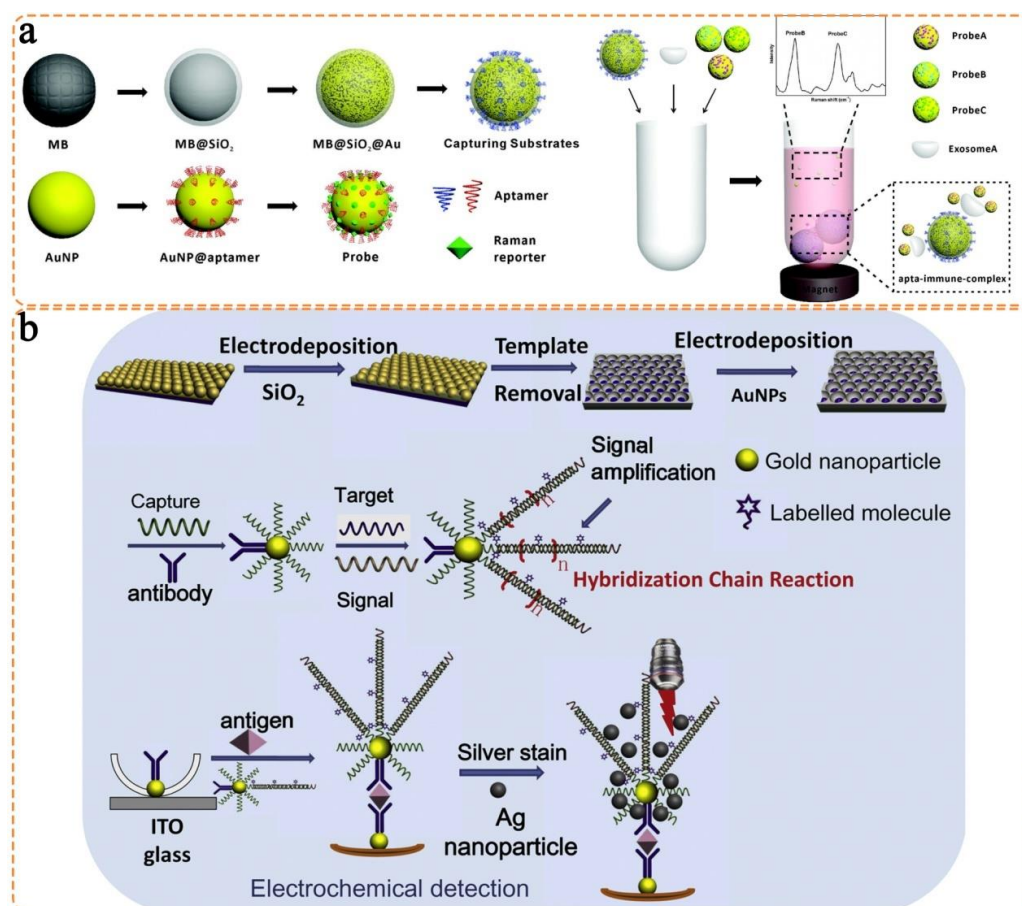


Figure 5. Gold nanosphere-based SERS nanotags for parallel biomarker detection. (a) Detection of three EVs together with magnetic nanobeads using the prepared three SERS nanotags (i.e., Probe A, Probe B, and Probe C). Reproduced with permission [49]. Copyright 2018, Royal Society of Chemistry. (b) Supersensitive detection of two circulating protein biomarkers by coupling with silver nanospheres to further enhance the signals and using hybridization chain reaction to improve the sensitivity. Reproduced with permission [50]. Copyright 2021, Elsevier.

3.2. Anisotropic Nanostructures

Compared to the above-mentioned isotropic nanostructures, anisotropic nanostructures feature greatly enhanced electromagnetic fields on specific sites with high curvature (e.g., tips and corners on the nanostructure surfaces). This property produces “hot spots” that are able to significantly amplify Raman signals. Currently, a series of anisotropic nanostructures have been investigated to enable highly sensitive cancer circulating biomarker detection.

Gold nanostar, which has extremely strong “hot spots” on the tips or branches, is a typical and widely used anisotropic nanostructure in SERS assay. For instance, Li and coworkers et al. architected gold nanostar-based SERS nanotags for breast cancer diagnosis by detecting three circulating antigen biomarkers (i.e., cancer antigen (CA) 15-3, CA 27–29, and CEA) (Figure 6a) [51]. In this work, an assay chip with pre-defined wells was functionalized with antibodies to capture the targets. The sequential addition of targets and gold nanostar-based SERS nanotags formed an immune sandwich structure for detection. Due to gold nanostar-enabled enormous Raman signal enhancement, this assay outperformed the traditional immunoassays and allowed the sensitive detection of three biomarkers down to 0.99 U/mL, 0.13 U/mL, and 0.05 ng/mL for CA15-3, CA27-29, and CEA, respectively. Simulated patient sample tests were conducted by spiking the targets into healthy human serum. Though this work can readout three biomarkers, the target identification was based on the spatial differentiation instead of the intrinsic Raman signal labeling.

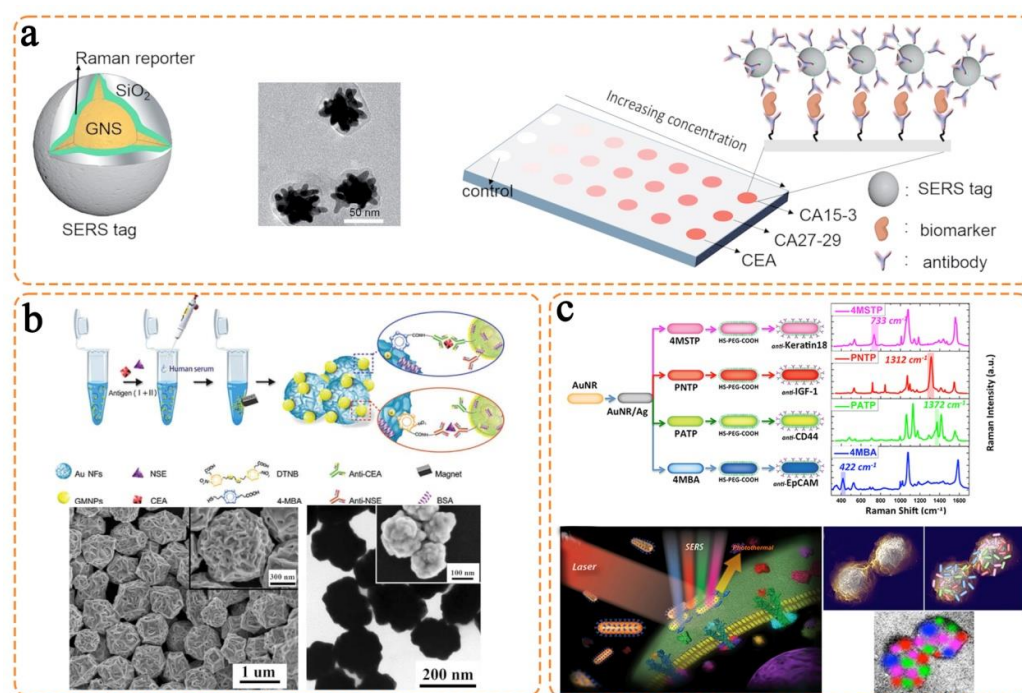


Figure 6. Anisotropic nanostructure-based SERS nanotags for parallel detection of multiple circulating biomarkers. (a) Gold nanostars as plasmonic nanostructures to detect three breast cancer antigens (i.e., CEA, CA27-29, and CA15-3). Reproduced with permission [51]. Copyright 2015, Royal Society of Chemistry. (b) Gold nanoflowers allowing the parallel and sensitive detection of two lung cancer-associated biomarkers (i.e., NSE and CEA) with the scanning electron microscope (SEM) and transmission electron microscope (TEM) images showing the morphology of gold nanoflowers. Reproduced with permission. Copyright 2016, Royal Society of Chemistry [52]. (c) Silver-gold nanorods promoting multi-color and multi-mode detection of biomarkers (i.e., Keratin18, IGF-1, CD44, and EpCAM) on breast cancer CTCs. Reproduced with permission [53]. Copyright 2014, Nature Publishing Group.

As a similar structure to nanostars, nanoflowers show strong “hot spots” on the protrusions and thus are efficient SERS plasmonic nanostructures. Song and colleagues synthesized gold nanoflowers and achieved lung cancer-associated circulating protein biomarker detection (Figure 6b) [52]. Using a traditional SERS nanotag preparation method, the gold nanoflowers were coated with two Raman reporters and corresponding antibodies. Using the magnetic nanoparticles to separate the targets (i.e., CEA and neuron-specific enolase (NSE)), the gold nanoflower-based SERS nanotags were further applied to identify the targets and enabled the readout of characteristic Raman signals for intensity-based quantification. As the gold nanoflowers possessed a higher Raman signal enhancement than the traditional gold nanospheres, this work demonstrated the sensitive detection of CEA and NSE in human serum with the limit of detection of 1.48 pg/mL and 2.04 pg/mL, respectively. Given that the plasmonic nanostructures with the optimal SERS enhancement possess a size below 100 nm, gold nanoflowers with a size of ~750 nm in this work can be reduced to a smaller size by optimizing the synthetic conditions to further improve the analytical performance.

Nanorod is another class of commonly used plasmonic nanostructures in SERS assay. Nima et al. designed silver–gold nanorod SERS nanotags for multicolor breast cancer CTC identification (Figure 6c) [53]. Specifically, to prepare the SERS nanotags, gold nanorods were first coated with a silver layer that produced electromagnetic coupling to improve Raman enhancement, followed by conjugating Raman reporters and antibodies on the surfaces. The prepared SERS nanotags targeted four surface biomarkers on breast CTCs, namely Keratin18, insulin-like growth factor (IGF), CD44, and EpCAM. Significantly, this

silver–gold nanorod SERS assay achieved the highly sensitive and specific detection of single breast CTCs in unprocessed human blood. In addition to acting as SERS plasmonic nanostructures, the silver–gold nanorods were further used as photothermal agents for rapid screening. Thus, the silver–gold nanorods underpinned multi-biomarker and multi-mode detection, which had the potential to improve the currently available complex CTC analysis.

In addition, the nanobox is attracting more attention as a powerful SERS plasmonic nanostructure for a range of circulating biomarkers' detection, such as proteins, EVs, and CTCs. Li and colleagues first synthesized gold–silver alloy nanoboxes and demonstrated the single-particle SERS activity [54]. On the basis of this, they integrated nanobox-based SERS nanotags with a nanopillar array for a digital analysis of four cytokines (Figure 7a) [55]. In this work, the nanopillar array with dimensions of $1000\text{ nm} \times 1000\text{ nm} \times 1000\text{ nm}$ was designed to capture the individual cytokines by following Poisson distribution. The single-particle active SERS nanotags then allowed the readout of the cytokine binding events under confocal Raman microscope. Due to the optimization of the nanopillar height, the nonspecific binding events were largely screened from the confocal signal detection, which partly improved the assay specificity and sensitivity. Furthermore, unlike the conventional quantification with SERS intensity, this nanobox-based digital platform relied on the “yes/no” readout mode to count the targets. Such a novel design ensured the detection sensitivity to the single-molecule level and avoided the potential SERS signal fluctuation bias due to nanostructure aggregation. Importantly, this nanobox-based SERS digital assay allowed the monitoring of melanoma patients receiving immune checkpoint therapy.

Following the cytokine detection, the nanobox-based SERS nanotags and the nanopillar array were further extended into profiling EVs to differentiate malignant and benign lung cancer (Figure 7b) [56]. Specifically, under Poisson distribution, individual EVs were captured on the nanopillar array and identified by the nanobox-based SERS nanotags. The EV molecular profile consisting of four biomarkers (i.e., CD63, thrombospondin 2 (THBS2), versican (VCAN), and tenascin C (TNC)) was established to correlate with lung lesions. In a patient cohort of 33 participants, the EV molecular profile allowed the identification of malignant from benign with the area under the curve of 0.85, suggesting the possibility of this tool in performing noninvasive lung cancer screening.

Moreover, nanobox-based SERS nanotags can be used to detect melanoma CTC signatures for predicting the response of immune checkpoint blockade therapy (Figure 7c) [57]. To obtain a unique CTC signature, nanobox-based SERS nanotags were prepared to target four biomarkers on melanoma CTCs, namely programmed cell death-ligand 1 (PD-L1), major histocompatibility (MHC)-I/II, and MCSP. The nanobox-based SERS nanotags enabled a simultaneous ensemble and single-cell level profiling of melanoma CTCs. Thus, this work provided a comprehensive CTC phenotype with the ability to reveal cancer heterogeneity. By comparing the CTC molecular profile changes before and after interferon- γ stimulation, this work showcased the identification of immune checkpoint blockade responders in a cohort of 14 melanoma patients. Furthermore, with the aid of magnetic beads for target separation and purification, the nanobox-based SERS nanotags were also applied for multiplexed soluble cancer protein biomarker detection, which was able to fulfill the sensitivity requirement of patient screening in clinical settings [58]. Taking all the evidence together, the nanoboxes showed their capability as promising SERS plasmonic nanostructures in multiplexed cancer circulating biomarker detection.

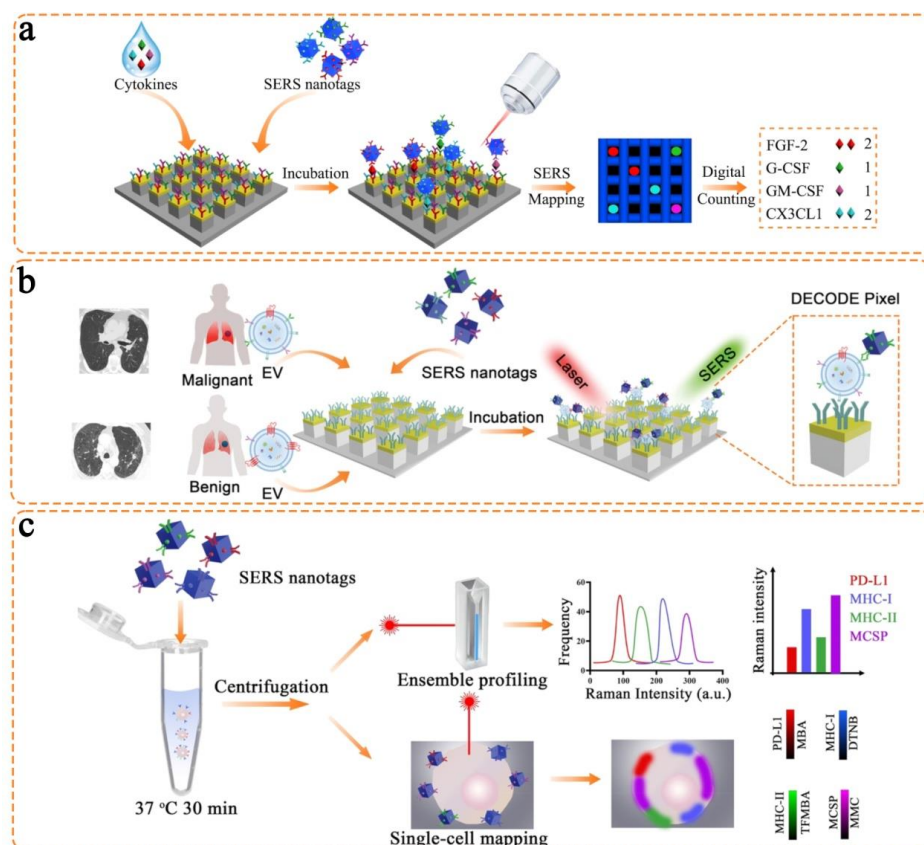


Figure 7. Gold–silver alloy nanobox-based SERS nanotags for a variety of cancer biomarker detection. (a) The integration with the nanopillar array for digital counting of four cytokines (i.e., FGF-2, G-CSF, GM-CSF, and CX3CL1). Reproduced with permission [55]. Copyright 2021, Nature Publishing Group. (b) Digital assay to measure four lung cancer-associated EV biomarkers for differentiating malignant and benign lung cancers. Reproduced with permission [56]. Copyright 2022, Wiley-VCH. (c) Profiling of four biomarkers on melanoma CTCs (i.e., PD-L1, MHC-I, MHC-II, and MCSP). Reproduced with permission [57]. Copyright 2022, American Chemical Society.

4. Triple Bond-Modulated Raman Reporters in SERS Nanotags for Multi-Biomarker Detection

Though the traditional Raman reporters allow the multi-biomarker labeling, their multiplexing capability is restricted by the spectral overlap due to the rich vibrational and rotational information in the Raman fingerprint region. To further expand Raman multiplexing labeling, Min and coworkers pioneered the triple bond molecules as supermultiplex Raman reporters. Particularly, they developed the Manhattan Raman scattering (MARS) dyes (Figure 8a) and polyyne-based molecules termed as “carbon rainbow” with tunable Raman shifts (Figure 8b) [27,59,60]. In contrast to the traditional Raman reporters, the triple bond molecules featured simple Raman peaks in the Raman silent region, thereby less likely to produce overlapping peaks with other molecules. Due to this advantage, the triple bond molecules showed broad applications in multiplexed biological imaging, live cell profiling, and volumetric mapping [61–63]. However, their usage was typically performed with stimulated Raman scattering (SRS) to amplify the weak Raman signals, which necessitated the employment of state-of-the-art equipment for detection. Recently, accumulating investigations have demonstrated triple bond molecules as effective Raman reporters in SERS assay.

With the assistance of density functional theory calculation, Chen et al. designed and synthesized an alkyne-modulated palette with 16 molecules derived from 4-mercaptobenzoic acid, 4-ethynylbenzenethiol, and 4-(buta-1,3-diyne) benzenethiol [64]. Their finding sug-

gested that the use of 4-ethynylbenzenethiol as a parent structure was only able to alter the alkynyl Raman shifts to a slight extent by using different substituents at the benzene ring (i.e., 2118 cm^{-1} to 2126 cm^{-1}). However, the Raman shifts demonstrated a wide range of changes with the addition of substituents to the terminal alkyne (i.e., 2118 cm^{-1} to 2238 cm^{-1}). Furthermore, the increase in charge density on the $\text{C} \equiv \text{C}$ led to the Raman shift towards a higher wavenumber due to the enhanced bond energy. Following these fundamental investigations, three alkyne-containing molecules with clearly separated signals (i.e., 2105 cm^{-1} , 2159 cm^{-1} , and 2212 cm^{-1}) were selected as representative Raman reporters to prepare SERS nanotags, in which gold–silver nanospheres were used as plasmonic nanostructures (Figure 9a). As a proof-of-concept demonstration, the three SERS nanotags allowed the labeling of three targets on HeLa cells, showing the optical interference-free advantage. This work can be further extended into profiling multiple biomarkers on CTC surfaces.

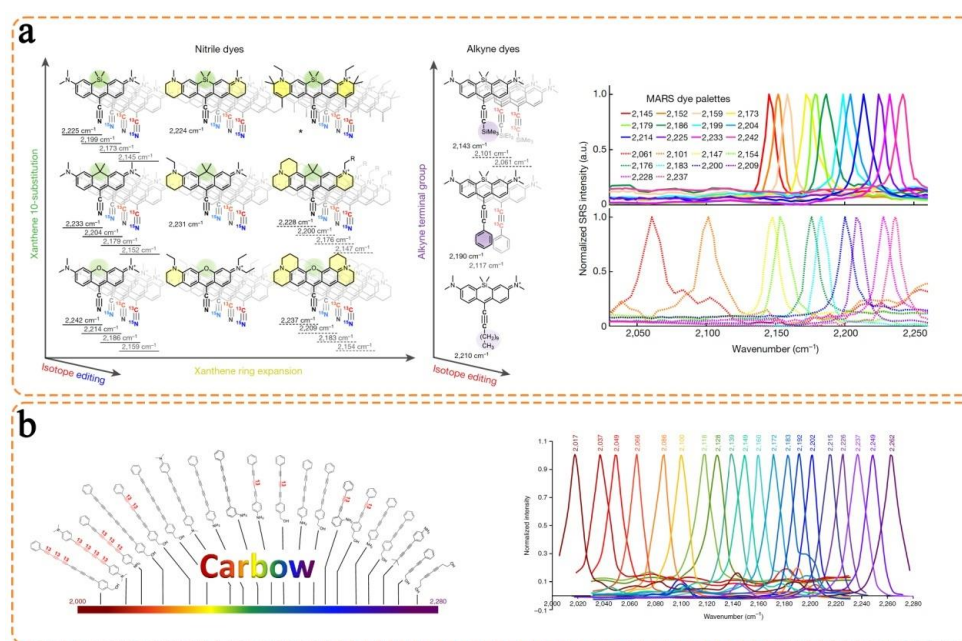


Figure 8. Designing the triple bond-modulated molecules as emerging Raman reporters to improve the multiplexing capability. (a) 9-Cyanopyronin-based MARS dyes to adjust Raman shift through Xanthene ring expansion, isotope editing, and alkyne terminal group control. Reproduced with permission [27]. Copyright 2017, Nature Publishing Group. (b) Polyynes-based “carbon rainbow” dyes with tunable Raman shift from 2000 cm^{-1} to 2280 cm^{-1} . Reproduced with permission [60]. Copyright 2019, Nature Publishing Group.

Following the previous investigation of an alkyne-modulated palette, Bai et al. used triple bond molecules (i.e., $\text{C} \equiv \text{N}$ and $\text{C} \equiv \text{C}$) as Raman reporters to simultaneously label three liver cancer-associated antigens: AFP, CEA, and ferritin (FER) (Figure 9b) [65]. In this work, three triple bond molecules were designed to correlate with the three antigens, respectively. Specifically, the triple bond molecules and antibodies were co-conjugated to gold nanospheres as SERS nanotags, which produced well-separated Raman peaks at 2105 cm^{-1} , 2159 cm^{-1} , and 2227 cm^{-1} , respectively. After the three biomarkers were isolated from serum by magnetic beads, the prepared SERS nanotags were applied to further identify and readout specific signals. Due to the use of these triple bond molecules, this assay avoided the potential interferences from human serum that produced Raman signals in the fingerprint region. Importantly, the test on 39 clinical samples using this assay produced consistent results as the hospital diagnosis. Thus, this work demonstrated the potential of triple bond molecules as useful Raman reporters in future circulating biomarker detection.

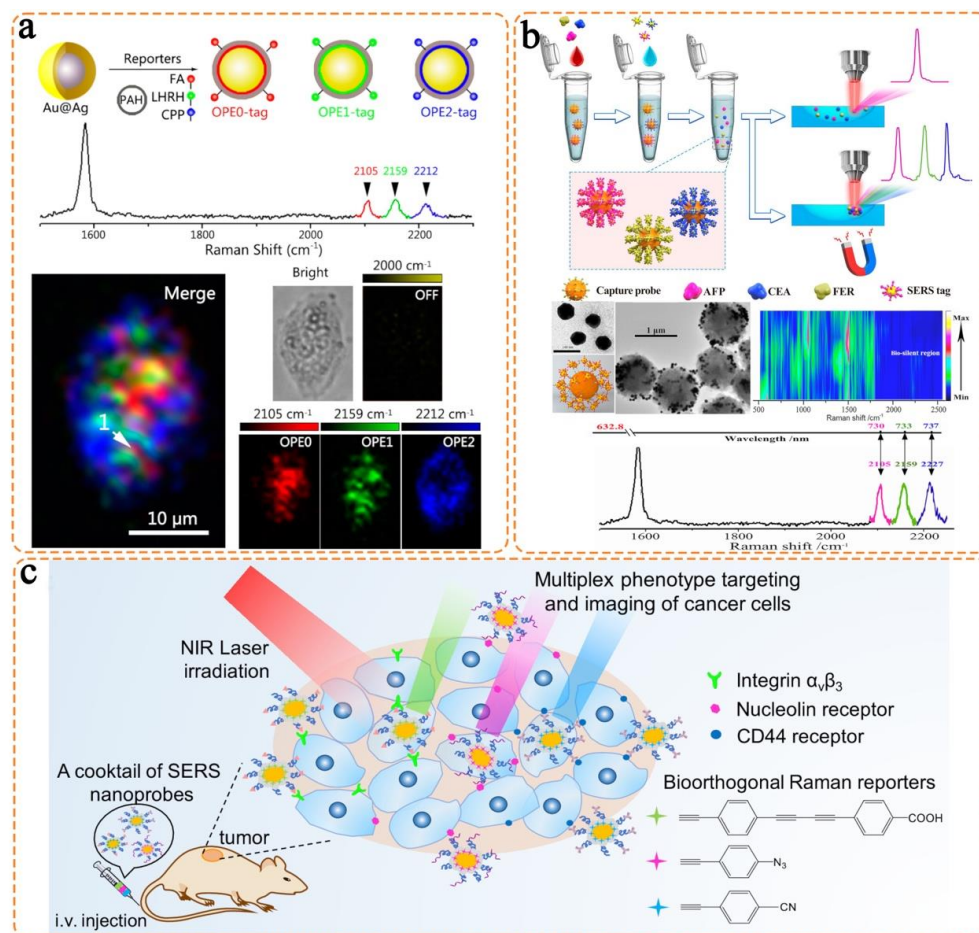


Figure 9. Triple bond-modulated molecules as Raman reporters in SERS nanotags for biomarker detection. (a) Three alkyne-containing molecules labeling surface receptors on HeLa cells (i.e., FA, LHRH, and CPP). Reproduced with permission [64]. Copyright 2016, American Chemical Society. (b) Three triple bond-containing molecules detecting specific liver cancer antigens (i.e., AFP, CEA, and FER). Reproduced with permission [65]. Copyright 2019, American Chemical Society. (c) Three triple bond-containing molecules for breast cancer phenotype detection by detecting three proteins on CTC surfaces (i.e., integrin $\alpha_v\beta_3$, nucleolin receptor, and CD44 receptor). Reproduced with permission [66]. Copyright 2019, American Chemical Society.

Furthermore, Wang et al. utilized three triple bond-containing molecules as Raman reporters to detect breast cancer phenotype and demonstrated their *in vivo* usage (Figure 8c) [66]. In their work, the SERS nanotags were prepared by coating the diynyl, azide, and cyano-containing molecules with characteristic Raman peaks (i.e., 2205 cm⁻¹, 2120 cm⁻¹, and 2230 cm⁻¹) and corresponding target ligands onto gold nanoflowers. The SERS nanotags allowed the phenotype differentiation of two breast cancer cell lines (i.e., MDA-MB-231 and MCF-7). Importantly, without the interference from biological components, the *in vivo* SERS detection showed identifiable Raman signals in the micro-tumor, which indicated the possibility of early cancer phenotype detection. This work thus highlighted the nonoverlap, high sensitivity, and background-free advantages of triple bond-modulated SERS nanotags.

Similarly, Li and colleagues demonstrated the use of alkyne- and nitrile-containing molecules as Raman reporters to prepare SERS nanotags and perform multi-color imaging of cancer cells and human breast cancer tissues [67]. There are also some reports demonstrating triple bond-based molecules in ion or inflammatory biomarker detection. Taken together, all the evidence indicates the prospects and progress of triple bond-based molecules in biosensing applications.

5. Challenges and Outlooks

In the preceding parts, we detailed the design principle of SERS nanotags as well as the use of SERS nanotags with different nanostructure morphologies and triple bond-modulated Raman reporters in circulating biomarker detection. Compared with the traditional biochemical assays (e.g., electrochemical and fluorescence tests), the SERS nanotag-enabled biomarker detection demonstrates an outstanding advantage of simultaneously measuring multiple targets due to the extremely narrow Raman linewidths. The representative works using different SERS nanotags are summarized in Table 2. Despite the favorable analytical performance in these studies (e.g., high sensitivity and specificity), the ultimate application of SERS nanotags in cancer detection still faces several challenges, particularly for use in clinical settings. In this section, we provide insight into the possible challenges and outlooks of SERS nanotags in multiplexed detection of circulating biomarkers, aiming to transit this technology into clinical use.

Table 2. Representative SERS nanotags in circulating biomarker detection.

Plasmonic Nanostructure	Reporter	Detected Biomarker	Samples	Application	Ref.
Gold nanospheres	<ul style="list-style-type: none"> 4-mercaptobenzoic acid (MBA) 2,3,5,6-tetrafluoro-4-mercaptobenzoic acid (TFMBA) 4-mercapto-3-nitro benzoic acid (MNBA) 4-mercaptopyridine (MPY) 	<ul style="list-style-type: none"> Melanoma-chondroitin sulfate proteoglycan (MCSP) Melanoma cell adhesion molecule (MCAM) Erythroblastic leukemia viral oncogene homologue 3 (ErbB3) Low-affinity nerve growth factor receptor (LNGFR) 	Human serum	Melanoma cancer detection and treatment monitoring	[44]
Gold nanospheres	<ul style="list-style-type: none"> 5,5-dithiobis (2-nitrobenzoic acid) (DTNB) MBA TFMBA MPY 	<ul style="list-style-type: none"> EpCAM E-cadherin N-cadherin ATP-binding cassette subfamily B member 5 (ABCB5) 	Human serum	Breast cancer metastasis monitoring	[45]
Silver-gold nanorods	<ul style="list-style-type: none"> MBA p-aminothiophenol (PATP) p-nitrothiophenol (PNTP) 4-(methylsulfanyl) thiophenol (4MSTP) 	<ul style="list-style-type: none"> EpCAM CD44 Keratin 18 Insulin-like growth factor antigen (IGF-1) 	Human blood	Breast cancer detection	[53]
Gold-silver alloy nanoboxes	<ul style="list-style-type: none"> DTNB MBA TFMBA MMTAA 	<ul style="list-style-type: none"> Fibroblast growth factor 2 (FGF-2) Granulocyte colony-stimulating factor (G-CSF) Granulocyte-macrophage colony-stimulating factor (GM-CSF) Fractalkine (CX3CL1) 	Human serum	Melanoma cancer treatment monitoring	[55]

Table 2. Cont.

Plasmonic Nanostructure	Reporter	Detected Biomarker	Samples	Application	Ref.
Gold nanospheres	<ul style="list-style-type: none"> • 4-Cyanobenzenethiol • OPE0 • OPE2 	<ul style="list-style-type: none"> • AFP • CEA • FER 	Human serum	Liver cancer detection	[65]
Gold nanoflowers	<ul style="list-style-type: none"> • Methyl 4-(4-ethynylphenylbuta-1,3-diyne-1-yl)benzoate acid • 4-Ethynylphenylacetone nitrile • 4-Ethynylphenylazide 	<ul style="list-style-type: none"> • Oligonucleotide aptamer (AS1411) • Cyclic arginine–glycine–aspartic acid (cRGD) • CD44 	Human cell lines and mice	Breast cancer detection	[66]

5.1. Improve the Nanostructure Reproducibility and Stability

To ensure the successful application of SERS nanotags in cancer detection, the first criterion is to produce accurate signal readouts with sufficient reproducibility. As the signal is highly dependent on the electromagnetic field enhancement, the preparation of uniform nanostructures from batch to batch is essential. Furthermore, the freshly prepared nanostructures may have the required stability in the beginning. In practice, the nanostructure is susceptible to aggregate in buffer solutions, which normally happens during the functionalization of Raman reporters or targeting units on nanostructure surfaces [68,69]. The nanostructure aggregation can cause significant variations in SERS signals because of the random “hot spots” produced in the aggregates. Thus, more effective approaches to prepare highly stable nanostructures that can endure multiple steps of functionalization should be investigated. Moreover, the facile one-step functionalization or one-pot synthesis and modification strategies should also be developed to reduce the aggregation issue in the future.

5.2. Explore New Strategies to Tune the Raman Shifts of Triple Bond-Modulated Raman Reporters

Currently, the triple bond-modulated molecules allow an easier separation of Raman peaks from each other in the Raman silent region, which is the major advantage compared to the molecules with Raman signals in the fingerprint region. Although different strategies have been used to tune their Raman shifts (e.g., introducing heavy atoms), the practical synthesis of a series of triple bond-modulated molecules is still difficult. To enable convenient and widespread use of triple bond-modulated Raman reporters, exploring new approaches that allow an easier control of Raman shifts are desired [70,71]. For instance, the test of a library of molecular structures that have flexible vibration and rotation can be a good starting point [72]. The subsequent applications can select the molecules allowing easier synthesis.

5.3. Promote Broad Collaborations

SERS is a technology that involves multidisciplinary knowledge. Specifically, the synthesis of nanostructures relies on material scientists to ensure the controllable morphology and strong Raman signal enhancement [73–75]. The achievement of characteristic Raman spectra with non-overlapping signals requires organic synthetic scientists to rationally design novel molecular structures [76,77]. Furthermore, the final application of SERS assay to perform various biomarker detection necessitates researchers from analytical chemistry [78,79]. Taking these thoughts into consideration, the successful SERS application should promote broad collaborations among researchers with different areas of expertise.

5.4. Realizing SERS with Multifunctional Abilities for Multimodal Imaging and Theranostics

Raman imaging holds the merits of multiple analyses and demonstrates the disadvantages of sensitivity and resolution. It is well known that the frontier fluorescence imaging and photoacoustic imaging modalities, especially in the NIR region, display in vivo imaging in deep tissue with high sensitivity and resolution (Figure 10) [80–82]. Therefore, the combination of other molecular imaging modalities with SERS will undoubtedly overcome the limitation of each imaging modality [83–85]. On the other hand, the integration of Raman imaging and photo/thermal/chemotherapy modalities could achieve precise image-guided therapy or imaging monitoring of therapeutic performance [86–88]. For example, the combination of gold/silver nanoparticles with small-molecule Raman reporters could be easily applied to construct multifunctional probes for in vivo cancer diagnosis and therapy [89,90]. Therefore, many effects should be considered to design novel multifunctional imaging agents based on the SERS for future in vivo theranostics with high-quality imaging figures and therapeutic performance.

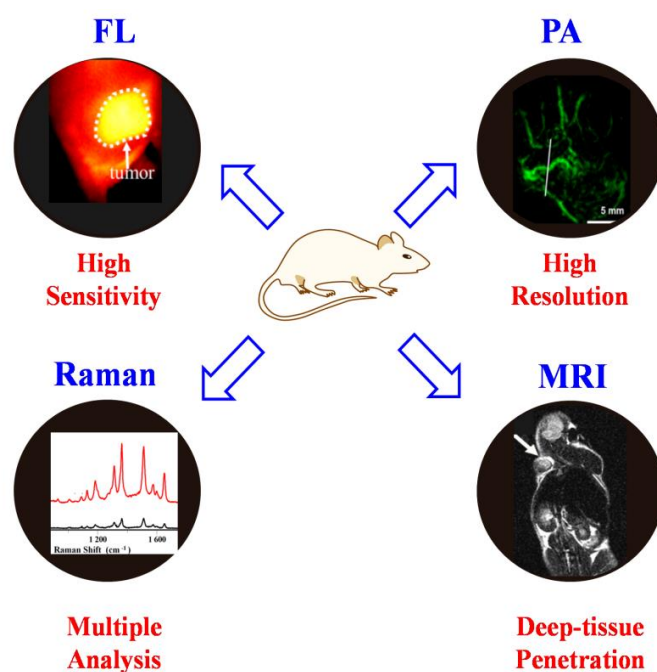


Figure 10. The advantages of each imaging modality.

5.5. Integration of SERS with Other Imaging or Therapy Modalities toward Precision Medicine

Because of the high sensitivity and intrinsic fingerprint spectrum, SERS nanotags have attracted much attention for in vivo and intraoperative imaging. Recently, in vivo fluorescence imaging and photoacoustic imaging in the second near-infrared (NIR-II) region have demonstrated remarkable advances with better spatial resolution and deeper tissue penetration than in the traditional visible and NIR-I regions [91–93]. The development of SERS nanotags at the NIR-II window is therefore highly valuable. The resonant strategy, i.e., the use of resonant substrates and resonant molecules, can be helpful in fabricating bright SERS nanotags at the NIR-II window; however, this strategy has not been demonstrated with sufficient quantitative assessments. Recently, Lin and coworkers reported a quantitative study on the Raman enhancements of the resonant strategy in preparing NIR-II SERS nanotags [94]. By comparing the resonant and nonresonant plasmonic nanorod substrates, the resonant substrates have been shown to provide an enhancement factor of up to four orders of magnitude. When using the resonant Raman reporter molecules, SERS intensities can be further increased by 25–546 times. This work opens a new strategy for fabricating ultrasensitive NIR-II SERS nanotags and provides insights into the design of related plasmonic devices in the future.

5.6. Test the Assay Performance on a Large Cohort of Clinical Samples

The ultimate goal of SERS assay is to shift from fundamental research into clinical use for cancer diagnosis. Admittedly, the current SERS assay reported acceptable analytical performance, with a low limit of detection and wide dynamic detection range. Most of the studies performed testing in buffer solutions or simulated patient samples. However, clinical samples are much more complex than the buffer system, with the existence of a high abundance of interfering molecules, which may lower the analytical performance and even lead to detection failure [95]. Therefore, the test of SERS assays on real samples is essential to allow the transition into clinical use. Though some works may try a few real samples, this is still far behind the required number of samples to achieve the transition to clinical settings. Therefore, our SERS assay can start by testing a relatively large patient cohort (e.g., 50 samples). Gradually, we can increase the recruited patient cohort to progress into a clinical trial.

5.7. Pushing SERS Nanoprobes from In Vitro to In Vivo Applications

SERS technology is extremely sensitive and specific, can be multiplexed, and exhibits less photo-bleaching as compared to fluorescence [96]. Therefore, SERS is desirable for the development of non-invasive in vivo diagnostic and imaging tools. Compared with traditional imaging modalities such as MRI, FL, and PA, SERS imaging can provide high-resolution and molecular information for biomarkers at a lower cost. For example, recent research has confirmed that gold nanomaterials such as gold nanoparticles, gold nanostars, and gold nanorods are promising Raman substrates with outstanding surface plasmon resonance effects, adjustable structure, and adequate biocompatibility, making them widely used as SERS nanoprobes for in vivo diagnosis and imaging [97]. Though several types of gold nanomaterial-based SERS nanoprobes have been successfully applied for in vivo applications, the in vivo biocompatibility, sensitivity, and specificity still need to be improved. On the other hand, the SERS technique should also be integrated with other imaging techniques such as fluorescence/photoacoustic imaging. Finally, to speed up the in vivo applications of SERS imaging probes, specific attention should be paid to develop SERS probes in the NIR-II region.

6. Conclusions

As SERS is a powerful technology, in this work, we detailed SERS-based assays for the highly sensitive detection of multiple circulating biomarkers in parallel. In particular, we featured the use of SERS nanotags as the core for biomarker detection. We fully discussed the basic design principle of SERS nanotags, highlighting the four major components (i.e., plasmonic nanostructure, Raman reporter, protective shell, and targeting unit). Following that, we focused on the SERS nanotags that used two types of plasmonic nanostructures and triple bond-modulated Raman reporters in circulating biomarker detection. We also present our opinions on the challenges and outlooks of SERS-based assays in cancer diagnosis. We hope this review can guide the rational design of novel types of SERS nanotags and expand their applications in multiplexed biomarker detection for accurate cancer detection in vitro and in vivo.

Author Contributions: Conceptualization, Y.S. and J.L.; writing—original draft preparation, Z.Z. and R.G.; writing—review and editing, Y.S. and J.L.; supervision, Y.S. All authors have read and agreed to the published version of the manuscript.

Funding: We acknowledge the financial support from the National Natural Science Foundation of China (22204055, 22022404, 22074050) and the Natural Science Foundation of Hubei Province (2022CFA033); the Fundamental Research Funds for the Central Universities (CCNU22QN007), supported by the Open Project Program of Key Laboratory for Analytical Science of Food Safety and Biology, Ministry of Education (FS2202); the Open Project Program of Hubei Province Key Laboratory of Occupational Hazard Identification and Control, Wuhan University of Science and Technology (OHIC2022K02); and the Open Project Program of Key Laboratory of Optic-electric Sensing and Analytical Chemistry for Life Science (M2022-5), MOE.

Institutional Review Board Statement: Not applicable.

Informed Consent Statement: Not applicable.

Data Availability Statement: Not applicable.

Conflicts of Interest: The authors declare no conflict of interest.

Abbreviations

SERS	surface-enhanced Raman scattering	CTCs	circulating tumor cells
NAs	nucleic acids	EVs	extracellular vesicles
PSA	prostate-specific antigen	BSA	bovine serum albumin
LSPR	localized surface plasma resonance	MCSP	melanoma–chondroitin sulfate proteoglycan
MCAM	melanoma cell adhesion molecule	EpCAM	epithelial cell adhesion molecule
EMT	mesenchymal transition	EHD	electrohydrodynamic
CEA	carcinoembryonic antigen	HER2	human epidermal growth factor receptor 2
AFP	alpha-fetoprotein	GMA	microelectrode array
HCR	hybridization chain reaction	CA	cancer antigen
SEM	scanning electron microscope	TEM	transmission electron microscope
NSE	neuron-specific enolase	IGF	insulin-like growth factor
THBS2	thrombospondin 2	VCAN	versican
TNC	tenascin C	PD-L1	programmed cell death-ligand 1
MHC	major histocompatibility	MARS	Manhattan Raman scattering
SRS	stimulated Raman scattering	MBA	4-mercaptobenzoic acid
TFMBA	2,3,5,6-tetrafluoro-4-mercaptobenzoic acid	MNBA	4-mercapto-3-nitro benzoic acid
MPY	4-mercaptopyridine	DTNB	5,5-dithiobis(2-nitrobenzoic acid)
PATP	p-aminothiophenol	PNTP	p-nitrothiophenol
4MSTP	4-(methylsulfanyl)thiophenol	FGF-2	fibroblast growth factor 2
G-CSF	granulocyte colony-stimulating factor	AS1411	oligonucleotide aptamer
cRGD	cyclic arginine–glycine–aspartic acid	FL	fluorescence imaging
PA	photoacoustic imaging		

References

- World Health Organization (WHO). Cancer. 2022. Available online: <https://www.who.int/news-room/fact-sheets/detail/cancer> (accessed on 3 February 2022).
- Borrebaeck, C.A.K. Precision diagnostics: Moving towards protein biomarker signatures of clinical utility in cancer. *Nat. Rev. Cancer* **2017**, *17*, 199. [[CrossRef](#)] [[PubMed](#)]
- Koo, K.M.; Wee, E.J.H.; Mainwaring, P.N.; Wang, Y.; Trau, M. Toward precision medicine: A cancer molecular subtyping nano-strategy for RNA biomarkers in tumor and urine. *Small* **2016**, *12*, 6233–6242. [[CrossRef](#)] [[PubMed](#)]
- Xu, Y.; Li, C.; Ma, X.; Tuo, W.; Tu, L.; Li, X.; Sun, Y.; Stang, P.J.; Sun, Y. Long wavelength-emissive Ru(II) metallacycle-based photosensitizer assisting in vivo bacterial diagnosis and antibacterial treatment. *Proc. Natl. Acad. Sci.* **2022**, *119*, e2209904119. [[CrossRef](#)] [[PubMed](#)]
- Shi, G.; Zhong, M.; Ye, F.; Zhang, X. Low-frequency HIFU induced cancer immunotherapy: Tempting challenges and potential opportunities. *Cancer Bio. Med.* **2019**, *16*, 714. [[CrossRef](#)]
- Crowley, E.; Di Nicolantonio, F.; Loupakis, F.; Bardelli, A. Liquid biopsy: Monitoring cancer-genetics in the blood. *Nat. Rev. Clin. Oncol.* **2013**, *10*, 472. [[CrossRef](#)]
- Li, J.; Wuethrich, A.; Dey, S.; Lane, R.E.; Sina, A.A.I.; Wang, J.; Wang, Y.; Puttick, S.; Koo, K.M.; Trau, M. The growing impact of micro/nanomaterial-based systems in precision oncology: Translating “multiomics” technologies. *Adv. Funct. Mater.* **2020**, *30*, 1909306. [[CrossRef](#)]
- Wang, T.; Li, J.; Yu, G.; Yu, K. Effects of siRNA interference and over-expression of HMGA2 on proliferation and apoptosis of colorectal cancer cells. *Int. J. Clin. Exp. Pathol.* **2017**, *10*, 4611.
- Li, W.; Wang, H.; Zhao, Z.; Gao, H.; Liu, C.; Zhu, L.; Wang, C.; Yang, Y. Emerging nanotechnologies for liquid biopsy: The detection of circulating tumor cells and extracellular vesicles. *Adv. Mater.* **2018**, *31*, 1805344. [[CrossRef](#)] [[PubMed](#)]
- Duan, R.; Zhang, Z.; Zheng, F.; Wang, L.; Guo, J.; Zhang, T.; Dai, X.; Zhang, S.; Yang, D.; Kuang, R.; et al. Combining protein and miRNA quantification for bladder cancer analysis. *ACS Appl. Mater. Interfaces* **2017**, *9*, 23420–23427. [[CrossRef](#)]

11. Liu, C.; Xu, X.; Li, B.; Situ, B.; Pan, W.; Hu, Y.; An, T.; Yao, S.; Zheng, L. Single-exosome-counting immunoassays for cancer diagnostics. *Nano Lett.* **2018**, *18*, 4226–4232. [[CrossRef](#)]
12. Ning, Z.; Gan, J.; Chen, C.; Zhang, D.; Zhang, H. Molecular functions and significance of the MTA family in hormone-independent cancer. *Cancer Metast. Rev.* **2014**, *33*, 901. [[CrossRef](#)] [[PubMed](#)]
13. Li, Y.Q.; Chandran, B.K.; Lim, C.T.; Chen, X. Rational design of materials interface for efficient capture of circulating tumor cells. *Adv. Sci.* **2015**, *2*, 1500118. [[CrossRef](#)] [[PubMed](#)]
14. Li, J.; Wang, J.; Wang, Y.; Trau, M. Simple and rapid colorimetric detection of melanoma circulating tumor cells using bifunctional magnetic nanoparticles. *Analyst* **2017**, *142*, 4788–4793. [[CrossRef](#)]
15. Bostwick, D.G. Prostate-specific antigen. Current role in diagnostic pathology of prostate cancer. *Am. J. Clin. Pathol.* **1994**, *102*, S31–S37. [[PubMed](#)]
16. Ankerst, D.P.; Thompson, I.M. Sensitivity and specificity of prostate-specific antigen for prostate cancer detection with high rates of biopsy verification. *Arch. Ital. Urol. Androl.* **2006**, *78*, 125–129.
17. Ferrari, M. Cancer nanotechnology: Opportunities and challenges. *Nat. Rev. Cancer* **2005**, *5*, 161–171. [[CrossRef](#)]
18. Langer, J.; Jimenez de Aberasturi, D.; Aizpurua, J.; Alvarez-Puebla, R.A.; Auguie, B.; Baumberg, J.J.; Bazan, G.C.; Bell, S.E.J.; Boisen, A.; Brolo, A.G.; et al. Present and future of surface-enhanced Raman scattering. *ACS Nano* **2020**, *14*, 28–117. [[CrossRef](#)]
19. Wang, Y.; Yan, B.; Chen, L. SERS tags: Novel optical nanoprobes for bioanalysis. *Chem. Rev.* **2013**, *113*, 1391–1428.
20. Mir-Simon, B.; Reche-Perez, I.; Guerrini, L.; Pazos-Perez, N.; Alvarez-Puebla, R.A. Universal one-pot and scalable synthesis of SERS encoded nanoparticles. *Chem. Mater.* **2015**, *27*, 950–958. [[CrossRef](#)]
21. Tan, T.; Tian, C.; Ren, Z.; Yang, J.; Chen, Y.; Sun, L.; Li, Z.; Wu, A.; Yin, J.; Fu, H. LSPR-dependent SERS performance of silver nanoplates with highly stable and broad tunable LSPR prepared through an improved seed-mediated strategy. *Phys. Chem. Chem. Phys.* **2013**, *15*, 21034–21042. [[CrossRef](#)]
22. Im, H.; Bantz, K.C.; Lee, S.H.; Johnson, T.W.; Haynes, C.L.; Oh, S.-H. Self-assembled plasmonic nanoring cavity arrays for SERS and LSPR biosensing. *Adv. Mater.* **2013**, *25*, 2678–2685. [[CrossRef](#)] [[PubMed](#)]
23. Li, J.; Koo, K.M.; Wang, Y.; Trau, M. Native microRNA targets trigger self-assembly of nanozyme-patterned hollowed nanocuboids with optimal interparticle gaps for plasmonic-activated cancer detection. *Small* **2019**, *15*, 1904689. [[CrossRef](#)] [[PubMed](#)]
24. Jeon, T.Y.; Park, S.-G.; Lee, S.Y.; Jeon, H.C.; Yang, S.-M. Shape control of Ag nanostructures for practical sers substrates. *ACS Appl. Mater. Interfaces* **2013**, *5*, 243–248. [[CrossRef](#)] [[PubMed](#)]
25. Benz, F.; Chikkaraddy, R.; Salmon, A.; Ohadi, H.; de Nijs, B.; Mertens, J.; Carnegie, C.; Bowman, R.W.; Baumberg, J.J. SERS of individual nanoparticles on a mirror: Size does matter, but so does shape. *J. Phys. Chem. Lett.* **2016**, *7*, 2264–2269. [[CrossRef](#)]
26. Shen, X.S.; Wang, G.Z.; Hong, X.; Zhu, W. Nanospheres of silver nanoparticles: Agglomeration, surface morphology control and application as SERS substrates. *Phys. Chem. Chem. Phys.* **2009**, *11*, 7450–7454. [[CrossRef](#)]
27. Wei, L.; Chen, Z.; Shi, L.; Long, R.; Anzalone, A.V.; Zhang, L.; Hu, F.; Yuste, R.; Cornish, V.W.; Min, W. Super-multiplex vibrational imaging. *Nature* **2017**, *544*, 465–470. [[CrossRef](#)]
28. Zheng, X.-S.; Hu, P.; Cui, Y.; Zong, C.; Feng, J.-M.; Wang, X.; Ren, B. BSA-coated nanoparticles for improved SERS-based intracellular pH sensing. *Anal. Chem.* **2014**, *86*, 12250–12257. [[CrossRef](#)]
29. Indrasekara, A.S.D.S.; Paladini, B.J.; Naczynski, D.J.; Starovoytov, V.; Moghe, P.V.; Fabris, L. Dimeric gold nanoparticle assemblies as tags for SERS-based cancer detection. *Adv. Healthc. Mater.* **2013**, *2*, 1370–1376. [[CrossRef](#)]
30. Fales, A.M.; Yuan, H.; Vo-Dinh, T. Silica-coated gold nanostars for combined surface-enhanced Raman scattering (SERS) detection and singlet-oxygen generation: A potential nanopatform for theranostics. *Langmuir* **2011**, *27*, 12186–12190. [[CrossRef](#)]
31. Farahavar, G.; Abolmaali, S.S.; Nejatollahi, F.; Safaie, A.; Javanmardi, S.; Khajeh Zadeh, H.; Yousefi, R.; Nadgaran, H.; Mohammadi-Samani, S.; Tamaddon, A.M.; et al. Single-chain antibody-decorated Au nanocages@liposomal layer nanoprobes for targeted SERS imaging and remote-controlled photothermal therapy of melanoma cancer cells. *Mater. Sci. Eng. C* **2021**, *124*, 112086. [[CrossRef](#)]
32. Kumar, A.R.; Shanmugasundaram, K.B.; Li, J.; Zhang, Z.; Ibn Sina, A.A.; Wuethrich, A.; Trau, M. Ultrasensitive melanoma biomarker detection using a microchip sers immunoassay with anisotropic Au–Ag alloy nanoboxes. *RSC Adv.* **2020**, *10*, 28778–28785. [[CrossRef](#)] [[PubMed](#)]
33. Farokhinejad, F.; Li, J.; Hugo, L.E.; Howard, C.B.; Wuethrich, A.; Trau, M. Detection of dengue virus 2 with single infected mosquito resolution using yeast affinity bionanofragments and plasmonic sers nanoboxes. *Anal. Chem.* **2022**, *94*, 14177–14184. [[CrossRef](#)] [[PubMed](#)]
34. Berciaud, S.; Cognet, L.; Tamarat, P.; Lounis, B. Observation of intrinsic size effects in the optical response of individual gold nanoparticles. *Nano Lett.* **2005**, *5*, 515–518. [[CrossRef](#)] [[PubMed](#)]
35. Zhang, Y.; Walkenfort, B.; Yoon, J.H.; Schlucker, S.; Xie, W. Gold and silver nanoparticle monomers are non-sers-active: A negative experimental study with silica-encapsulated raman-reporter-coated metal colloids. *Phys. Chem. Chem. Phys.* **2015**, *17*, 21120–21126. [[CrossRef](#)]
36. Kleinman, S.L.; Frontiera, R.R.; Henry, A.-I.; Dieringer, J.A.; Van Duyne, R.P. Creating, characterizing, and controlling chemistry with sers hot spots. *Phys. Chem. Chem. Phys.* **2013**, *15*, 21–36. [[CrossRef](#)]
37. Willets, K.A. Super-resolution imaging of sers hot spots. *Chem. Soc. Rev.* **2014**, *43*, 3854–3864. [[CrossRef](#)]
38. Pearce, A.K.; Wilks, T.R.; Arno, M.C.; O'Reilly, R.K. Synthesis and applications of anisotropic nanoparticles with precisely defined dimensions. *Nat. Rev. Chem.* **2021**, *5*, 21–45. [[CrossRef](#)]

39. Sajanlal, P.R.; Sreeprasad, T.S.; Samal, A.K.; Pradeep, T. Anisotropic nanomaterials: Structure, growth, assembly, and functions. *Nano Rev.* **2011**, *2*, 5883. [[CrossRef](#)]
40. Mulvihill, M.J.; Ling, X.Y.; Henzie, J.; Yang, P. Anisotropic etching of silver nanoparticles for plasmonic structures capable of single-particle sensors. *J. Am. Chem. Soc.* **2010**, *132*, 268–274. [[CrossRef](#)]
41. Ye, S.; Benz, F.; Wheeler, M.C.; Oram, J.; Baumberg, J.J.; Cespedes, O.; Christenson, H.K.; Coletta, P.L.; Jeuken, L.J.; Markham, A.F. One-step fabrication of hollow-channel gold nanoflowers with excellent catalytic performance and large single-particle sensor activity. *Nanoscale* **2016**, *8*, 14932–14942. [[CrossRef](#)]
42. Tran, V.; Thiel, C.; Svejda, J.T.; Jalali, M.; Walkenfort, B.; Erni, D.; Schlücker, S. Probing the sensor brightness of individual nanoparticles, hollow Au/Ag nanoshells, Au nanostars and Au core/Au satellite particles: Single-particle experiments and computer simulations. *Nanoscale* **2018**, *10*, 21721–21731. [[CrossRef](#)] [[PubMed](#)]
43. Chang, H.; Kang, H.; Yang, J.-K.; Jo, A.; Lee, H.-Y.; Lee, Y.-S.; Jeong, D.H. Ag shell–Au satellite hetero-nanostructure for ultra-sensitive, reproducible, and homogeneous sensors activity. *ACS Appl. Mater. Interfaces* **2014**, *6*, 11859–11863. [[CrossRef](#)] [[PubMed](#)]
44. Tsao, S.C.-H.; Wang, J.; Wang, Y.; Behren, A.; Cebon, J.; Trau, M. Characterising the phenotypic evolution of circulating tumour cells during treatment. *Nat. Commun.* **2018**, *9*, 1482. [[CrossRef](#)]
45. Zhang, Z.; Wuethrich, A.; Wang, J.; Korbie, D.; Lin, L.L.; Trau, M. Dynamic monitoring of EMT in CTCs as an indicator of cancer metastasis. *Anal. Chem.* **2021**, *93*, 16787–16795. [[CrossRef](#)] [[PubMed](#)]
46. Kamil Reza, K.; Wang, J.; Vaidyanathan, R.; Dey, S.; Wang, Y.; Trau, M. Electrohydrodynamic-induced SERS immunoassay for extensive multiplexed biomarker sensing. *Small* **2017**, *13*, 1602902. [[CrossRef](#)]
47. Zhang, Z.; Wang, J.; Shanmugasundaram, K.B.; Yeo, B.; Möller, A.; Wuethrich, A.; Lin, L.L.; Trau, M. Tracking drug-induced epithelial–mesenchymal transition in breast cancer by a microfluidic surface-enhanced Raman spectroscopy immunoassay. *Small* **2020**, *16*, 1905614. [[CrossRef](#)] [[PubMed](#)]
48. Wang, J.; Wuethrich, A.; Sina, A.A.I.; Lane, R.E.; Lin, L.L.; Wang, Y.; Cebon, J.; Behren, A.; Trau, M. Tracking extracellular vesicle phenotypic changes enables treatment monitoring in melanoma. *Sci. Adv.* **2020**, *6*, eaax3223. [[CrossRef](#)] [[PubMed](#)]
49. Wang, Z.; Zong, S.; Wang, Y.; Li, N.; Li, L.; Lu, J.; Wang, Z.; Chen, B.; Cui, Y. Screening and multiple detection of cancer exosomes using an SERS-based method. *Nanoscale* **2018**, *10*, 9053–9062. [[CrossRef](#)]
50. Gu, X.; Wang, K.; Qiu, J.; Wang, Y.; Tian, S.; He, Z.; Zong, R.; Kraatz, H.-B. Enhanced electrochemical and SERS signals by self-assembled gold microelectrode arrays: A dual readout platform for multiplex immunoassay of tumor biomarkers. *Sens. Actuators B Chem.* **2021**, *334*, 129674. [[CrossRef](#)]
51. Li, M.; Kang, J.W.; Sukumar, S.; Dasari, R.R.; Barman, I. Multiplexed detection of serological cancer markers with plasmon-enhanced Raman spectro-immunoassay. *Chem. Sci.* **2015**, *6*, 3906–3914. [[CrossRef](#)]
52. Song, C.; Yang, Y.; Yang, B.; Min, L.; Wang, L. Combination assay of lung cancer associated serum markers using surface-enhanced Raman spectroscopy. *J. Mater. Chem. B* **2016**, *4*, 1811–1817. [[CrossRef](#)] [[PubMed](#)]
53. Nima, Z.A.; Mahmood, M.; Xu, Y.; Mustafa, T.; Watanabe, F.; Nedosekin, D.A.; Juratli, M.A.; Fahmi, T.; Galanzha, E.I.; Nolan, J.P.; et al. Circulating tumor cell identification by functionalized silver-gold nanorods with multicolor, super-enhanced SERS and photothermal resonances. *Sci. Rep.* **2014**, *4*, 4752. [[CrossRef](#)] [[PubMed](#)]
54. Li, J.; Zhang, G.; Wang, J.; Maksymov, I.S.; Greentree, A.D.; Hu, J.; Shen, A.; Wang, Y.; Trau, M. Facile one-pot synthesis of nanodot-decorated gold–silver alloy nanoboxes for single-particle surface-enhanced Raman scattering activity. *ACS Appl. Mater. Interfaces* **2018**, *10*, 32526–32535. [[CrossRef](#)] [[PubMed](#)]
55. Li, J.; Wuethrich, A.; Sina, A.A.I.; Cheng, H.-H.; Wang, Y.; Behren, A.; Mainwaring, P.N.; Trau, M. A digital single-molecule nanopillar SERS platform for predicting and monitoring immune toxicities in immunotherapy. *Nat. Commun.* **2021**, *12*, 1087. [[CrossRef](#)] [[PubMed](#)]
56. Li, J.; Sina, A.A.I.; Antaw, F.; Fielding, D.; Möller, A.; Lobb, R.; Wuethrich, A.; Trau, M. Digital decoding of single extracellular vesicle phenotype differentiates early malignant and benign lung lesions. *Adv. Sci.* **2022**, *10*, 2204207. [[CrossRef](#)] [[PubMed](#)]
57. Li, J.; Wuethrich, A.; Zhang, Z.; Wang, J.; Lin, L.L.; Behren, A.; Wang, Y.; Trau, M. SERS multiplex profiling of melanoma circulating tumor cells for predicting the response to immune checkpoint blockade therapy. *Anal. Chem.* **2022**, *94*, 14573–14582. [[CrossRef](#)] [[PubMed](#)]
58. Li, J.; Wang, J.; Grewal, Y.S.; Howard, C.B.; Raftery, L.J.; Mahler, S.; Wang, Y.; Trau, M. Multiplexed SERS detection of soluble cancer protein biomarkers with gold–silver alloy nanoboxes and nanoyeast single-chain variable fragments. *Anal. Chem.* **2018**, *90*, 10377–10384. [[CrossRef](#)]
59. Miao, Y.; Qian, N.; Shi, L.; Hu, F.; Min, W. 9-Cyanopyronin probe palette for super-multiplexed vibrational imaging. *Nat. Commun.* **2021**, *12*, 4518. [[CrossRef](#)]
60. Hu, F.; Zeng, C.; Long, R.; Miao, Y.; Wei, L.; Xu, Q.; Min, W. Supermultiplexed optical imaging and barcoding with engineered polyynes. *Nat. Methods* **2018**, *15*, 194–200. [[CrossRef](#)]
61. Hu, F.; Shi, L.; Min, W. Biological imaging of chemical bonds by stimulated Raman scattering microscopy. *Nat. Methods* **2019**, *16*, 830–842. [[CrossRef](#)]
62. Chen, C.; Zhao, Z.; Qian, N.; Wei, S.; Hu, F.; Min, W. Multiplexed live-cell profiling with Raman probes. *Nat. Commun.* **2021**, *12*, 3405. [[CrossRef](#)] [[PubMed](#)]

63. Shi, L.; Wei, M.; Miao, Y.; Qian, N.; Shi, L.; Singer, R.A.; Benninger, R.K.P.; Min, W. Highly-multiplexed volumetric mapping with Raman dye imaging and tissue clearing. *Nat. Biotechnol.* **2022**, *40*, 364–373. [[CrossRef](#)] [[PubMed](#)]
64. Chen, Y.; Ren, J.-Q.; Zhang, X.-G.; Wu, D.-Y.; Shen, A.-G.; Hu, J.-M. Alkyne-modulated surface-enhanced Raman scattering-palette for optical interference-free and multiplex cellular imaging. *Anal. Chem.* **2016**, *88*, 6115–6119. [[CrossRef](#)] [[PubMed](#)]
65. Bai, X.-R.; Wang, L.-H.; Ren, J.-Q.; Bai, X.-W.; Zeng, L.-W.; Shen, A.-G.; Hu, J.-M. Accurate clinical diagnosis of liver cancer based on simultaneous detection of ternary specific antigens by magnetic induced mixing surface-enhanced Raman scattering emissions. *Anal. Chem.* **2019**, *91*, 2955–2963. [[CrossRef](#)] [[PubMed](#)]
66. Wang, J.; Liang, D.; Feng, J.; Tang, X. Multicolor cocktail for breast cancer multiplex phenotype targeting and diagnosis using bioorthogonal surface-enhanced Raman scattering nanoprobe. *Anal. Chem.* **2019**, *91*, 11045–11054. [[CrossRef](#)]
67. Li, M.; Wu, J.; Ma, M.; Feng, Z.; Mi, Z.; Rong, P.; Liu, D. Alkyne- and nitrile-anchored gold nanoparticles for multiplex SERS imaging of biomarkers in cancer cells and tissues. *Nanotheranostics* **2019**, *3*, 113–119. [[CrossRef](#)] [[PubMed](#)]
68. Lee, S.; Sun, Y.; Cao, Y.; Kang, S.H. Plasmonic nanostructure-based bioimaging and detection techniques at the single-cell level. *Trend Anal. Chem.* **2019**, *117*, 58–68. [[CrossRef](#)]
69. Lin, S.; Cheng, Z.; Li, Q.; Wang, R.; Yu, F. Toward Sensitive and Reliable Surface-Enhanced Raman Scattering Imaging: From Rational Design to Biomedical Applications. *ACS Sens.* **2012**, *6*, 3912–3932. [[CrossRef](#)] [[PubMed](#)]
70. Eremina, O.E.; Czaja, A.T.; Fernando, A.; Aron, A.; Eremin, D.B.; Zavaleta, C. Expanding the Multiplexing Capabilities of Raman Imaging to Reveal Highly Specific Molecular Expression and Enable Spatial Profiling. *ACS Nano* **2022**, *16*, 10341–10353. [[CrossRef](#)]
71. Zhong, Q.; Zhang, R.; Yang, B.; Tian, T.; Zhang, K.; Liu, B. A Rational Designed Bioorthogonal Surface-Enhanced Raman Scattering Nanoprobe for Quantitatively Visualizing Endogenous Hydrogen Sulfide in Single Living Cells. *ACS Sens.* **2022**, *7*, 893–899. [[CrossRef](#)]
72. Dodo, K.; Fujita, K.; Sodeoka, M. Raman Spectroscopy for Chemical Biology Research. *J. Am. Chem. Soc.* **2022**, *144*, 19651–19667. [[CrossRef](#)] [[PubMed](#)]
73. Zhang, W.; Yang, X.; Wu, G.; Cheng, L. Controlled Self-Assembly of Metallacycle -Bridged Gold Nanoparticles for Surface-Enhanced Raman Scattering. *Chem. Eur. J.* **2020**, *26*, 11695–11700. [[CrossRef](#)] [[PubMed](#)]
74. Xie, L.; Gong, K.; Liu, Y.; Zhang, L. Strategies and Challenges of Identifying Nanoplastics in Environment by Surface-Enhanced Raman Spectroscopy. *Environ. Sci. Technol.* **2023**, *57*, 25–43. [[CrossRef](#)]
75. Wu, G.; Zheng, W.; Yang, X.; Liu, Q.; Cheng, L. Supramolecular metallacycle-assisted interfacial self-assembly: A promising method of fabricating gold nanoparticle monolayers with precise interparticle spacing for tunable SERS activity. *Tetrahedron Lett.* **2022**, *94*, 153716. [[CrossRef](#)]
76. Morsby, J.J.; Thimes, R.L.; Olson, J.E.; McGarraugh, H.H.; Payne, J.N.; Camden, J.P.; Smith, B.D. Enzyme Sensing Using 2-Mercaptopyridine-Carbonitrile Reporters and Surface-Enhanced Raman Scattering. *ACS Omega* **2022**, *7*, 6419–6426. [[CrossRef](#)]
77. Li, M.; Tian, S.; Meng, F.; Yin, M.; Yue, Q.; Wang, S.; Bu, W.; Luo, L. Continuously Multiplexed Ultrastrong Raman Probes by Precise Isotopic Polymer Backbone Doping for Multidimensional Information Storage and Encryption. *Nano Lett.* **2022**, *22*, 4544–4551. [[CrossRef](#)] [[PubMed](#)]
78. Plou, J.; Valera, P.S.; Garcia, I.; de Albuquerque, C.D.L.; Carracedo, A.; Liz-Marzan, L.M. Prospects of Surface-Enhanced Raman Spectroscopy for Biomarker Monitoring toward Precision Medicine. *ACS Photonics* **2022**, *9*, 333–350. [[CrossRef](#)] [[PubMed](#)]
79. Li, J.; Liu, F.; Ye, J. Boosting the Brightness of Thiolated Surface-Enhanced Raman Scattering Nanoprobes by Maximal Utilization of the Three-Dimensional Volume of Electromagnetic Fields. *J. Phys. Chem. Lett.* **2022**, *13*, 6496–6502. [[CrossRef](#)] [[PubMed](#)]
80. Huang, W.; Yang, H.; Hu, Z.; Fan, Y.; Guan, X.; Feng, W.; Liu, Z.; Sun, Y. Rigidity Bridging Flexibility to Harmonize Three Excited-State Deactivation Pathways for NIR-II-Fluorescent-Imaging-Guided Phototherapy. *Adv. Healthc. Mater.* **2021**, *10*, 2101003. [[CrossRef](#)]
81. Yang, H.; Tu, L.; Li, J.; Bai, S.; Hu, Z.; Yin, P.; Lin, H.; Yu, Q.; Zhu, H.; Sun, Y. Deep and precise lighting-up/combat diseases through sonodynamic agents integrating molecular imaging and therapy modalities. *Coordin. Chem. Rev.* **2022**, *453*, 214333.
82. Sun, Y.; Ding, F.; Chen, Z.; Zhang, R.; Li, C.; Xu, Y.; Zhang, Y.; Ni, R.; Li, X.; Yang, G.; et al. Melanin-dot-mediated delivery of metallacycle for NIR-II/photoacoustic dual-modal imaging-guided chemo-photothermal synergistic therapy. *Proc. Nat. Acad. Sci. USA* **2019**, *116*, 16729–16735. [[CrossRef](#)] [[PubMed](#)]
83. Tuo, W.; Xu, Y.; Fan, Y.; Li, J.; Qiu, M.; Xiong, X.; Li, X.; Sun, Y. Biomedical applications of Pt(II) metallacycle/metallacycle-based agents From mono-chemotherapy to versatile imaging contrasts and theranostic platforms. *Coordin. Chem. Rev.* **2021**, *443*, 214017. [[CrossRef](#)]
84. Li, Q.; Ge, X.; Ye, J.; Li, Z.; Su, L.; Wu, Y.; Yang, H.; Song, J. Dual Ratiometric SERS and Photoacoustic Core-Satellite Nanoprobe for Quantitatively Visualizing Hydrogen Peroxide in Inflammation and Cancer. *Angew. Chem. Int. Ed.* **2021**, *60*, 7323–7332. [[CrossRef](#)] [[PubMed](#)]
85. Li, C.; Xu, Y.; Tu, L.; Choi, M.; Fan, Y.; Chen, X.; Sessler, J.L.; Kim, J.S.; Sun, Y. Rationally designed Ru(II)-metallacycle chemo-phototheranostic that emits beyond 1000 nm. *Chem. Sci.* **2022**, *13*, 6541–6549. [[CrossRef](#)] [[PubMed](#)]
86. Xu, Y.; Li, C.; An, J.; Ma, X.; Yang, J.; Luo, L.; Deng, Y.; Kim, J.S.; Sun, Y. Construction of a 980 nm laser-activated Pt(II) metallacycle nanosystem for efficient and safe photo-induced bacteria sterilization. *Sci. China Chem.* **2023**, *66*, 155–163. [[CrossRef](#)]
87. Xu, Y.; Tuo, W.; Yang, L.; Sun, Y.; Li, C.; Chen, X.; Yang, W.; Yang, G.; Stang, P.J.; Sun, Y. Design of a Metallacycle-Based Supramolecular Photosensitizer for In Vivo Image-Guided Photodynamic Inactivation of Bacteria. *Angew. Chem. Int. Ed.* **2022**, *61*, e202110048.

88. Tu, L.; Li, C.; Liu, C.; Bai, S.; Yang, J.; Zhang, X.; Xu, L.; Xiong, X.; Sun, Y. Rationally designed Ru(II) metallacycles with tunable imidazole ligands for synergistical chemo-phototherapy of cancer. *Chem. Commun.* **2022**, *58*, 9068–9071. [[CrossRef](#)]
89. Henry, A.; Sharma, B.; Cardinal, M.F.; Kurouski, D.; van Duyne, R.P. Surface-Enhanced Raman Spectroscopy Biosensing: In Vivo Diagnostics and Multimodal Imaging. *Anal. Chem.* **2016**, *88*, 6638–6647. [[CrossRef](#)]
90. Chen, Z.; Mas, J.; Forbes, L.H.; Andrews, M.R.; Dholakia, K. Depth-resolved multimodal imaging: Wavelength modulated spatially offset Raman spectroscopy with optical coherence tomography. *J. Biophotonics* **2018**, *11*, e201700129. [[CrossRef](#)]
91. Zhang, X.; Li, C.; Zhang, Y.; Guan, X.; Mei, L.; Feng, H.; Li, J.; Tu, L.; Feng, G.; Deng, G.; et al. Construction of Long-Wavelength Emissive Organic Nanosensitizer Targeting Mitochondria for Precise and Efficient In Vivo Sonotherapy. *Adv. Funct. Mater.* **2022**, *32*, 2207259. [[CrossRef](#)]
92. Fan, Y.; Li, C.; Bai, S.; Ma, X.; Yang, J.; Guan, X.; Sun, Y. NIR-II Emissive Ru(II) Metallacycle Assisting Fluorescence Imaging and Cancer Therapy. *Small* **2022**, *18*, 2201625. [[CrossRef](#)]
93. Li, C.; Guan, X.; Zhang, X.; Zhou, D.; Son, S.; Xu, Y.; Deng, M.; Guo, Z.; Sun, Y.; Kim, J.S. NIR-II bioimaging of small molecule fluorophores: From basic research to clinical applications. *Biosen. Bioelec.* **2022**, *216*, 114620. [[CrossRef](#)] [[PubMed](#)]
94. He, H.; Zhang, Y.; Zhu, S.; Ye, J.; Lin, L. Resonant Strategy in Designing NIR-II SERS Nanotags: A Quantitative Study. *J. Phys. Chem. C* **2022**, *126*, 12575–12581. [[CrossRef](#)]
95. Merone, G.M.; Tartaglia, A.; Locatelli, M.; D'Ovidio, C.; Rosato, E.; de Grazia, U.; Santavenere, F.; Rossi, S.; Savini, F. Analytical chemistry in the 21st century: Challenges, solutions, and future perspectives of complex matrices quantitative analyses in biological/clinical field. *Analytica* **2020**, *1*, 44–59. [[CrossRef](#)]
96. Wen, C.; Wang, L.; Liu, L.; Shen, X.; Chen, H. Surface-enhanced Raman Probes Based on Gold Nanomaterials for in vivo Diagnosis and Imaging. *Chem. Asian J.* **2022**, *17*, e202200014. [[CrossRef](#)] [[PubMed](#)]
97. Zeng, L.; Pan, Y.; Wang, S.; Wang, X.; Zhao, X.; Ren, W.; Lu, G.; Wu, A. Raman Reporter-Coupled Ag_{core}@Au_{shell} Nanostars for in Vivo Improved Surface Enhanced Raman Scattering Imaging and Near-infrared-Triggered Photothermal Therapy in Breast Cancers. *ACS Appl. Mater. Interfaces* **2015**, *7*, 16781–16791. [[CrossRef](#)] [[PubMed](#)]

Disclaimer/Publisher's Note: The statements, opinions and data contained in all publications are solely those of the individual author(s) and contributor(s) and not of MDPI and/or the editor(s). MDPI and/or the editor(s) disclaim responsibility for any injury to people or property resulting from any ideas, methods, instructions or products referred to in the content.